Project No. 037005

CECILIA

Central and Eastern Europe Climate Change Impact and Vulnerability Assessment

Specific targeted research project

1.1.6.3.I.3.2: Climate change impacts in central-eastern Europe

D3.3: Assessment of RCM and SDS models in the impact target areas by their validation according to relevant criteria; ranking of the models if possible

Due date of deliverable: 1 June 2008
Actual submission date: 30 December 2009

Start date of project: 1 June 2006   Duration: 36 months

Lead contractor for this deliverable: Institute of Atmospheric Physics (IAP)

Revision (final)

1. Introductory remarks

The goal of this deliverable is to evaluate the downscaling models, both dynamical and statistical, according to a common set of criteria. The contribution of partners to this deliverable is twofold: some partners (CUNI, IAP, CHMI) validate all the available models over a common domain in central Europe according a wide range of validation criteria; others (NMA, NIMH, OMSZ) concentrate on their specific methods and/or models and a subset of criteria in the impact target area of their interest.

2.1 Overview of CUNI, IAP, and CHMI activities for CECILIA D3.3

The validation activities of CUNI were concentrated on the assessment of downscaling techniques, both statistical and dynamical, for the region of the Czech Republic, and identification of the best approach or approaches. Selected additional tests have also been carried out for CECILIA validation domain (see deliverable D3.1). Pre-selected statistical methods were implemented, with a special emphasis to the nonlinear ones. Determination of the most suitable predictors and values of parameters was carried out. Along with the outcomes of statistical downscaling techniques, outputs of two ERA-40-driven regional climate models, RegCM and ALADIN, prepared in CECILIA WP2, were validated against a set of observed data from the Czech Republic as well as gridded observations. The target variables included daily mean, maximum and minimum temperature and daily precipitation. The validation statistics were selected to quantify the deterministic match of the observed and simulated data (root mean squared error, Pearson correlation coefficient), basic measures of position and spread of the statistical distributions (mean value, standard deviation), persistence of the time series (lag-1 autocorrelation) as well as a general match of the statistical distributions (chi^2 test-based score).

The comparison has shown a strong dependence of the results on the location of the measuring site and season/month. Overall, if a single method of downscaling is to be chosen for the area of the Czech Republic, the ALADIN model seems to produce the best or close-to-best results in most validation categories. With an aid from additional post-processing (removal of bias, variance increase, and correction for differences in altitude of real and model terrain), this model seems to provide satisfactory series of downscaled values of both temperature and precipitation. The RegCM model, while producing relatively realistic series of temperature-related characteristics, exhibits a very strong wet bias, sometimes almost doubling the average monthly precipitation sums. Further improvement of the RCM-generated data can be achieved by additional postprocessing, as shown in deliverable D3.2. The statistical downscaling techniques, especially the ones based on neural networks, seem to be fit for downscaling temperature (mean, maximum or minimum), but they produce unrealistically shaped statistical distributions of precipitation. The method of locally constant models does reproduce the statistical distributions of precipitation fairly well, but it is unable to capture the deterministic relation between large-scale predictors and local measurements (which is reflected in the low values of correlation between downscaled and observed data).

2.2: Downscaling methods

Five different statistical methods were applied, each embodying a different approach to construction of the transfer function between predictors and predictand. This versatility of the mappings should help to find the best mathematical representation of the relations between large-scale predictors and local measurements for each type of the target variable.

Multiple linear regression (MLP). This basic statistical method computes the target value of predictand as a linear combination of the predictors. The exact form of the transfer function (determined by the values of the regression coefficients) is chosen to minimize the mean squared error of the mapping.

Method of local linear models (LLM). Unlike MLR, this technique does not use linear models for the global description of the connections between predictors and predictand, but applies it individually for smaller regions of the space of predictors. Due to its local nature, LLM is well suited for capturing eventual nonlinear components of the relations.

Method of locally constant models (LCM). This technique approximates the value of predictand by the average value, corresponding to a certain number of the most similar situations in the history of the analyzed system. Based on the outcomes of preliminary tests, only a single most similar state was used here, effectively turning the LCM technique into the **method of analogues**. The similarity of different states was quantified by the Euclidian distance of the respective vectors of predictors.

3

Radial basis function neural network (RBF). This architecture of artificial neural network is based on the use radial transfer functions for the neurons in the network's hidden layer. Unlike for multilayer perceptrons (see below), no iterative learning is required. Positions of the Gaussian radial units were initialized by the randomly selected cases from the set of training data here.

Multilayer perceptron neural network (MLP) represents the most common type of artificial neural network, able to describe even complex nonlinear relations between inputs and target value(s). The networks used for downscaling here contained a single hidden layer with 20 neurons, with tanh activation functions. The network was trained by the iterative backpropagation algorithm in its basic form.

All statistical downscaling (SD) methods were applied with predictor data normalized to zero mean and identical standard deviation, for the period 1961-1990. The mappings were created for the series as a whole, without separating the individual seasons or months (while such separation was also experimented with, it generally only provided a small decrease of RMSE).

Along with the series generated by various techniques of statistical downscaling, outputs of two ERA-40 driven regional climate models (RCMs) were included in the comparison. These simulations were run for the CECILIA project by Charles University (model **RegCM**) and by the Czech Hydrometeorological Institute (model ALADIN-Climate/CZ, hereinafter referred to as **ALADIN**). The integration domains of both models were centered on Central Europe (Fig. 2.1), their basic horizontal resolution was about 10 km. Although there are other regional climate models run within the frame of CECILIA, they either do not cover the Czech Republic at all, or its territory lies too close to the edge of the model domain. For a more detailed description of the regional climate models, see the report for the CECILIA deliverable D2.1.
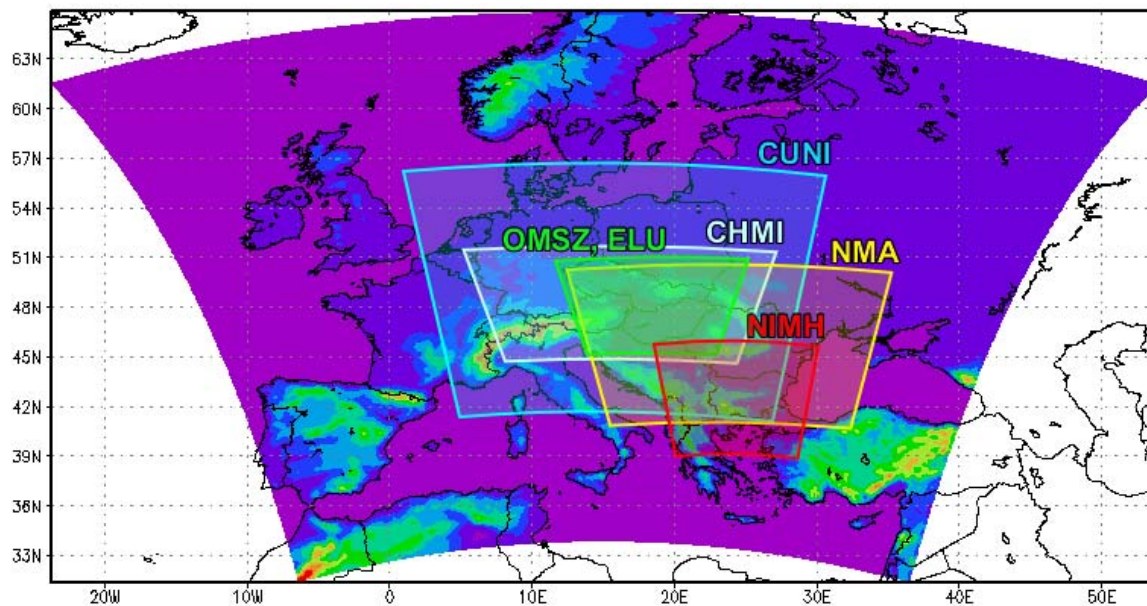

Fig. 2.1: Integration domains of CECILIA regional climate models. The two simulations employed for the present comparison are marked as CUNI (RegCM model run at Charles University) and CHMI (ALADIN-Climate/CZ of the Czech Hydrometeorological Institute). The colored area represents the domain of the ENSEMBLES project.

The series of the target variables were available in the temporal resolution of 3 h (RegCM) or 6 h (ALADIN) from the RCMs. Their conversion to daily data was done as follows:
- **Daily maximum (minimum) temperature** values were computed as maximum (minimum) values between 0:00 and 21:00 (18:00 for ALADIN) of the respective day (at Czech weather stations, the

values of maximum and minimum temperature are read daily at 21:00 of the local time of the respective meridian - HMÚ, 1972),

- **Mean daily temperature** was computed as an arithmetic average of values between 3:00 (6:00 for ALADIN) and 0:00 (at the weather stations, mean daily temperature is computed from temperatures at 7:00, 14:00 and 21:00 as $(T_7 + T_{14} + 2T_{21}) / 4$),

- **Daily precipitation** was computed as a sum of precipitation between 9:00 (12:00 for ALADIN) and 6:00 of the following day (daily precipitation totals are read at 7:00 of the local time at Czech weather stations).

2.3: Selection of predictors for statistical downscaling

ERA-40 reanalysis was used as the source of predictor series for statistical downscaling. Geopotential height, temperature, relative humidity and specific humidity from various pressure levels were tested in the role of potential predictors. After the preliminary tests, only temperature and geopotential height were kept as potential predictors for downscaling temperature; for precipitation, specific humidity was included as well. Because of the potentially worse match between 1000 hPa fields of the predictor variables in the reanalysis and in the global climate models, only variables from the 850 hPa and 500 hPa levels were used as potential predictors (i.e., variables representing the free atmosphere rather that the near-surface layer). The potential predictors were drawn from the area between 0° and 30°E and between 40°N and 60°N.

The actual selection of predictors was done individually for each combination of target variable and weather station. It was carried out by means of a simplified version of step-wise multiple linear regression, minimizing the out-of-sample RMSE. A fixed number of predictors ($M = 20$) was used for the final generation of downscaled series. This value of M was chosen after the tests with step-wise selection of predictors, which have shown that the decrease of RMSE ceases or becomes very slow before the dimension of the space of predictors exceeds approximately 20 (fig. 2.2).
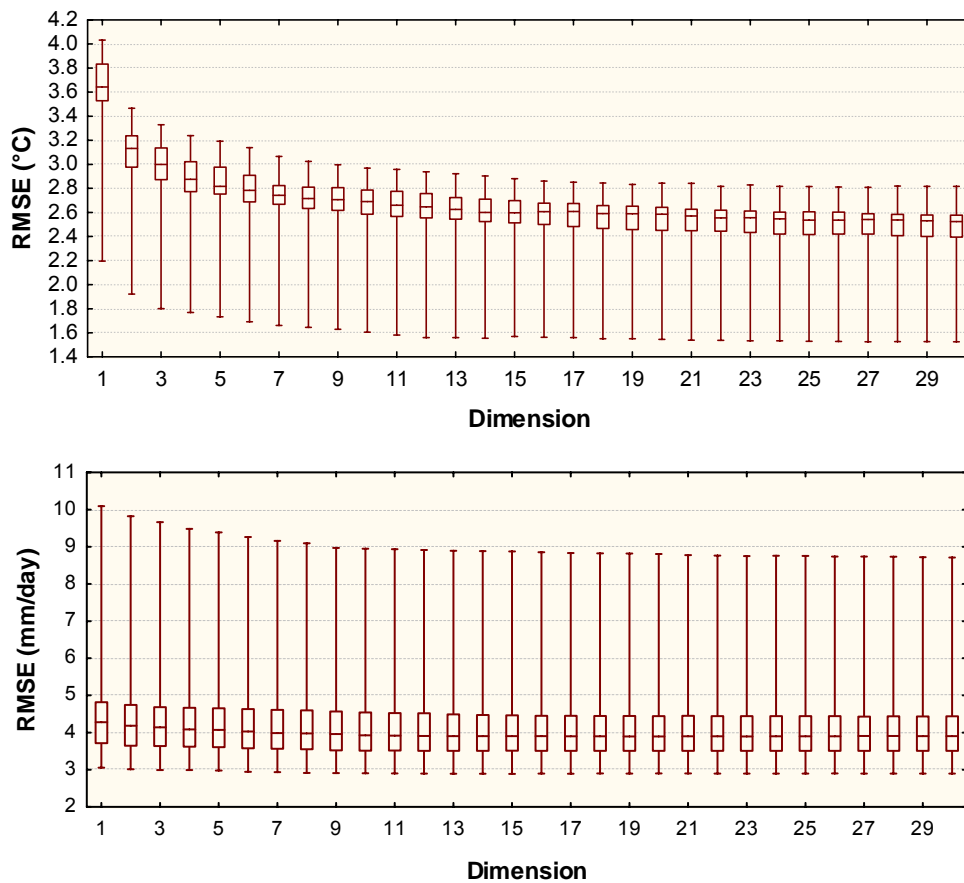
Fig. 2.2: RMSE of mean daily temperature (upper panel) and precipitation (lower panel) downscaling by multiple linear regression as a function of the number of predictors. The boxplots show distribution of values in the set of RMSEs for 25 Czech weather stations.

2.4: Determination of parameters for SD methods

Except for MLR, all used methods of statistical downscaling are generally nonlinear and they require the choice of the value of one or more parameters. These parameters determine the complexity of the mappings (e.g., number of neurons in the neural nets), the way in which the mapping is initialized (e.g., learning rate) and other characteristics. The most suitable values of the needed parameters were identified prior to generating the downscaled series, individually for each type of the target variable. To avoid the influence of overfitting and overtraining the mappings, the best combinations of parameters were chosen based on the values of out-of-sample root mean square error: The SDS techniques were calibrated for the period 1961-1990, the error was then computed for the years 1991-2000. Since it turned out that the optimum values of parameters were similar for all four types of target variables, a universal set of parameters could be used (table 2.1).

Note that the final validation, the results of which are shown in Sect. 2.7, was performed for the interval 1961-1990 only, and that data from this 30-year-long period were used for both calibration and testing of the mappings, to make the analysis consistent with the work on near future (2021-2050) and far future (2071-2100) time slices.

Table 2.1: Applied methods of statistical downscaling and values of needed parameters. Where multiple values of a parameter are given, the computation was carried out for all of them, and the one producing the lowest RMSE was employed for generating the final series. Training of MLPs was repeated three times and the realization giving the lowest RMSE was used.

Method	Acronym	Parameter	Value(s)
Multiple linear regression	MLP	-	-
Local linear models	LLM	Number of nearest neighbors	200, 400, 800
Locally constant models (analogues)	LCM	Number of nearest neighbors	1
Radial basis function neural network	RBF	Number of neurons	300
		Width of radial functions	50,100, 150, 200
Multilayer perceptron neural network	MLP	Number of neurons	20
		Learning rate	0.00001
		Number of learning epochs	1000

2.5 Validation criteria

No specialized impact-related criteria were applied, the validation was based on standard statistics, able to quantify the deterministic match of the downscaled and observed series, as well as the correspondence of their statistical distributions or temporal structure of the series. The following characteristics were computed for the entire period 1961-1990 as a whole and for individual months:
- **Mean value**,
- **Bias**, computed as a difference between simulated and observed means,
- **Standard deviation**,
- **Root mean squared error** (RMSE),
- **Pearson correlation coefficient**,
- **Lag-1 autocorrelation**, which was included as a linear measure of persistence, i.e., of the common information content of values close in time.

The strongly skewed distribution of daily precipitation cannot be sufficiently characterized by mean value and standard deviation alone. Therefore, a quantity was needed to evaluate the correspondence

of statistical distributions of values. Instead of employing a non-Gaussian parametric approximation, the fit of statistical distribution was quantified using a **chi[2] score**, based on the definition of the statistic of the χ^2 test:

$$\chi^2 = \sum_{i=1}^{M} \frac{\left(O_i - S_i\right)^2}{O_i}, \tag{2.1}$$

where O_i (S_i) represents the frequency of observed (simulated) precipitation in the i-th cathegory, $i = 1, \ldots, M$. The upper borders of the respective intervals were selected at values 0.1, 1, 2, 5, 10 and 20 mm for daily precipitation. The chi[2] quantity increases with the mismatch of occurrence of precipitation in individual categories, thus the values closest to zero indicate the best fit.

2.6 Validation data

A set of daily values of **mean, maximum and minimum air temperature** and **precipitation** from 25 Czech weather stations, operated by the Czech Hydrometeorological Institute, was employed for validating the downscaling results (fig. 2.3). The SD methods were used to directly reproduce the series recorded at the target site (i.e., the series of observations were used as predictands). In the case of RCMs, series from the grid point closest to the weather station was used for comparison with the measurements. Raw model outputs were considered, as well as series created by application of an elementary linear correction for the altitude difference

$$x_{\text{corrected}} = x + g\left(h_{\text{station}} - h_{\text{GP}}\right), \tag{2.2}$$

where g represents the mean vertical gradient of quantity x (computed over the entire period 1961-1990 for individual months, using all grid points of the respective model in the area covered by fig. 2.3). h_{station} and h_{GP} are altitudes of the station and of the nearest model gridpoint, respectively. A similar correction was also tested based on daily values of the vertical gradient (i.e., computed separately for each day). The outcomes were similar to using the mean monthly correction and they are not shown here. In sect. 2.7, the results derived from the altitude-corrected RCM outputs are denoted as RegCM-C and ALADIN-C, respectively.
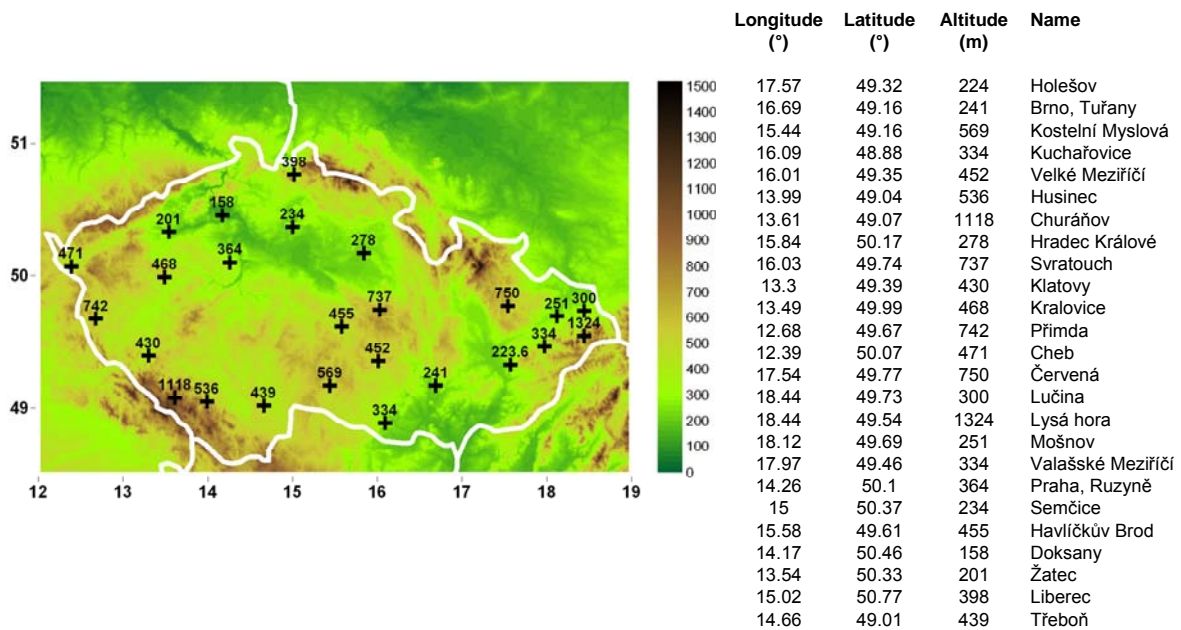

Longitude (°)	Latitude (°)	Altitude (m)	Name
17.57	49.32	224	Holešov
16.69	49.16	241	Brno, Tuřany
15.44	49.16	569	Kostelní Myslová
16.09	48.88	334	Kuchařovice
16.01	49.35	452	Velké Meziříčí
13.99	49.04	536	Husinec
13.61	49.07	1118	Churáňov
15.84	50.17	278	Hradec Králové
16.03	49.74	737	Svratouch
13.3	49.39	430	Klatovy
13.49	49.99	468	Kralovice
12.68	49.67	742	Přimda
12.39	50.07	471	Cheb
17.54	49.77	750	Červená
18.44	49.73	300	Lučina
18.44	49.54	1324	Lysá hora
18.12	49.69	251	Mošnov
17.97	49.46	334	Valašské Meziříčí
14.26	50.1	364	Praha, Ruzyně
15	50.37	234	Semčice
15.58	49.61	455	Havlíčkův Brod
14.17	50.46	158	Doksany
13.54	50.33	201	Žatec
15.02	50.77	398	Liberec
14.66	49.01	439	Třeboň

Fig. 2.3 Orography of the Czech Republic (m) with locations of the 25 stations used for the validation of SD/RCM outputs (left) and list of the stations (right). Source of the high-resolution orography data: U.S. Geological Survey (http://www.usgs.gov/).

2.7 Validation results

The results are sorted by the variable type, with a short overview at the beginning of each section (sects. 2.7.1 through 2.7.4). A summary evaluation of individual downscaling methods is then given in sect. 2.7.5. Because of the high number of combinations of variables/stations/seasons/criteria, most of the results are provided in the form of boxplots, created from the results for all 25 validation stations. In the case of precipitation (as the most difficult variable to downscale), some additional graphs are shown for station Holešov.

2.7.1 Daily mean temperature

The deviations of the monthly means of air temperature from the observed values are shown in fig. 2.4 for all methods and climatic seasons. It is clear that all techniques produce slightly biased series, but the magnitude of the difference varies with the station as well as season (for the year as a whole, MLR and RBF techniques are bias-free, as a result of the least-square optimization of the respective mappings). The bias and its changes during the year are also well detectable from the boxplots of monthly mean temperature in fig. 2.5. It is noteworthy that all methods, statistical and dynamical alike, exhibit a cold bias in spring. Since the driving data were obtained from the same reanalysis dataset, it can be speculated that this bias has been enforced by the character of ERA-40 data. It can also be mentioned that the SD methods were applied for the year as the whole, not individual seasons/months. Should the seasonalization be applied, the bias would be further reduced, but inhomogeneities could be introduced into the resulting series by the fact that different mappings (or, more precisely, sets of coefficients) would be used for different parts of the year. The relatively high warm bias of the RegCM and ALADIN models for some measuring sites (manifested as the extended positive tail of the boxplots) is caused by the presence of mountainous stations (especially Lysá hora and Chráňov) in the validation dataset, which are located much higher than the matching gridpoint of the RCMs. Application of a simple correction of the altitude difference (eq. 2.2) can reduce the severity of this problem (compare the boxplots marked as RegCM-C and ALADIN-C to those for raw model data, RegCM and ALADIN).

Both RCMs underestimate the dispersion of temperature values (fig. 2.6). For RegCM, the decreased variance is especially apparent in summer, for ALADIN in all seasons except autumn. In the case of SD methods, the standard deviation of temperature is typically more realistic, although the tendency for lower variance is also detectable (except for LCM, which overestimates the spread of values in some seasons).

The SD methods (except for LCM) give lower values of RMSE and higher correlation with series of observations than RCMs. However, this can be partly an effect of the choice of predictors, done to minimize RMSE of downscaling by linear regression. Also, especially in the case of MLP and RBF neural networks, mild overfitting of the mapping can play a role, due to the fact that the SD techniques were both calibrated and tested for the same interval.

Finally, all methods tend to produce series exhibiting slightly stronger persistence of values in all seasons but winter (fig. 2.9). The only exception is the LCM method, which generates series with much weaker autocorrelation than detected in the observed series.
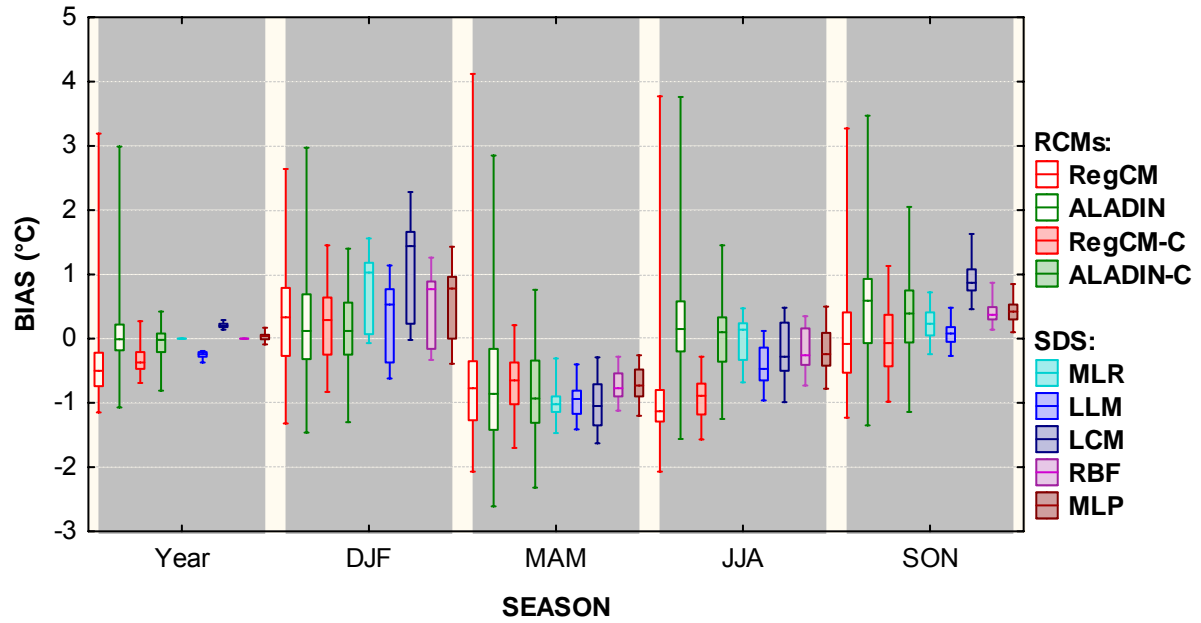
Fig. 2.4: Distribution of **mean daily temperature bias** for different methods of downscaling. The results for individual seasons are based on bias computed for separate months, for 25 Czech weather stations from fig. 2.3; the boxplots show minimum, q25, median, q75 and maximum values in the resulting set of 75 values.
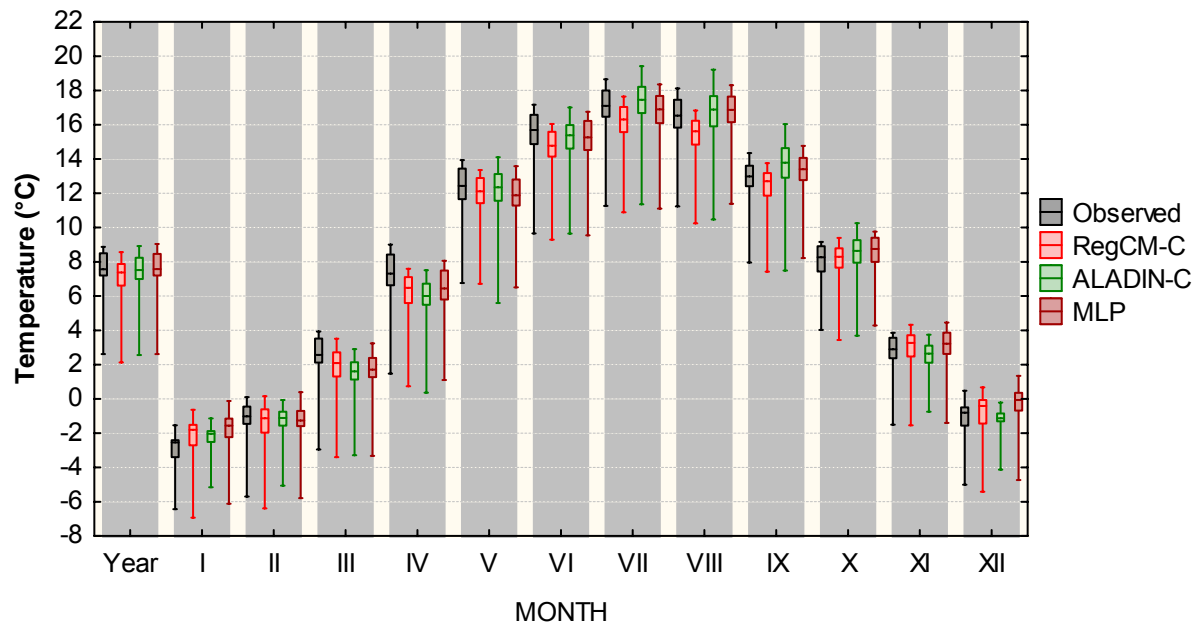

Fig. 2.5: Distribution of **monthly averages of mean daily temperature** for observed data and different methods of downscaling. The boxplots show minimum, q25, median, q75 and maximum values in the set of 25 Czech weather stations.
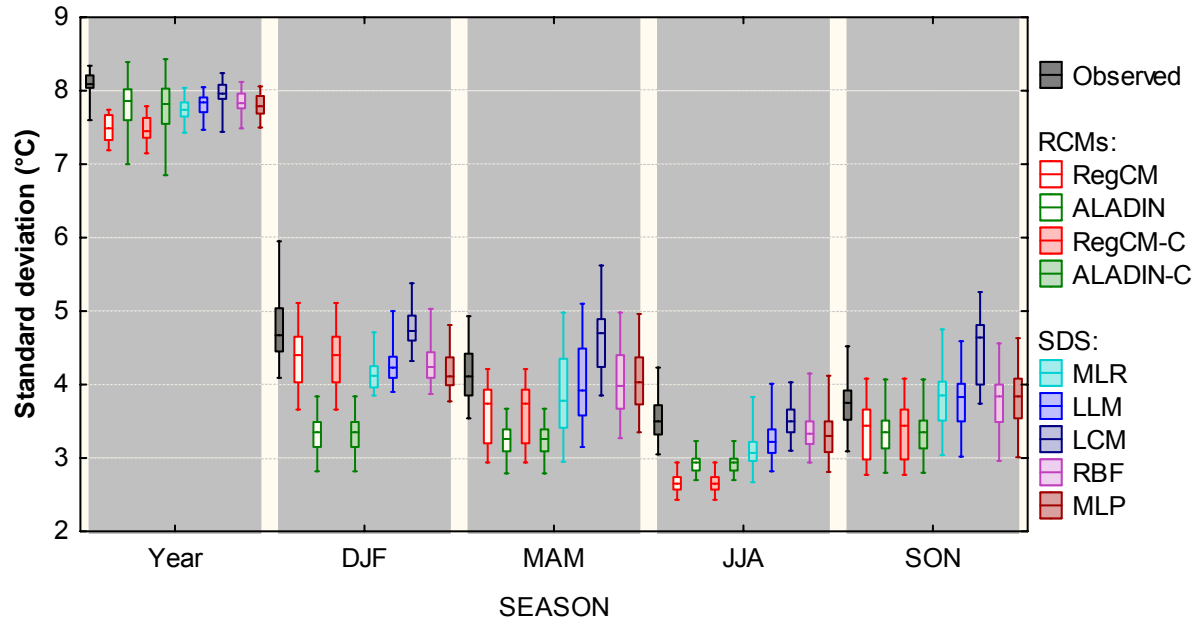
Fig. 2.6: Same as fig. 2.4, for **standard deviation of mean daily temperature.**
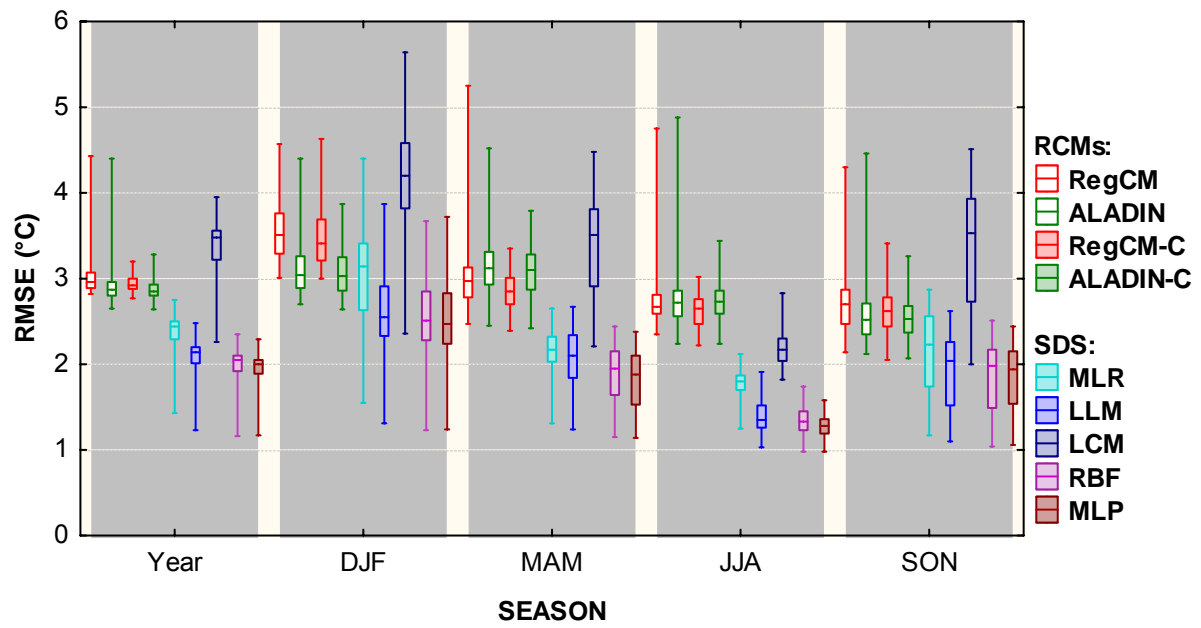
Fig. 2.7: Same as fig. 2.4, for **RMSE of mean daily temperature**.
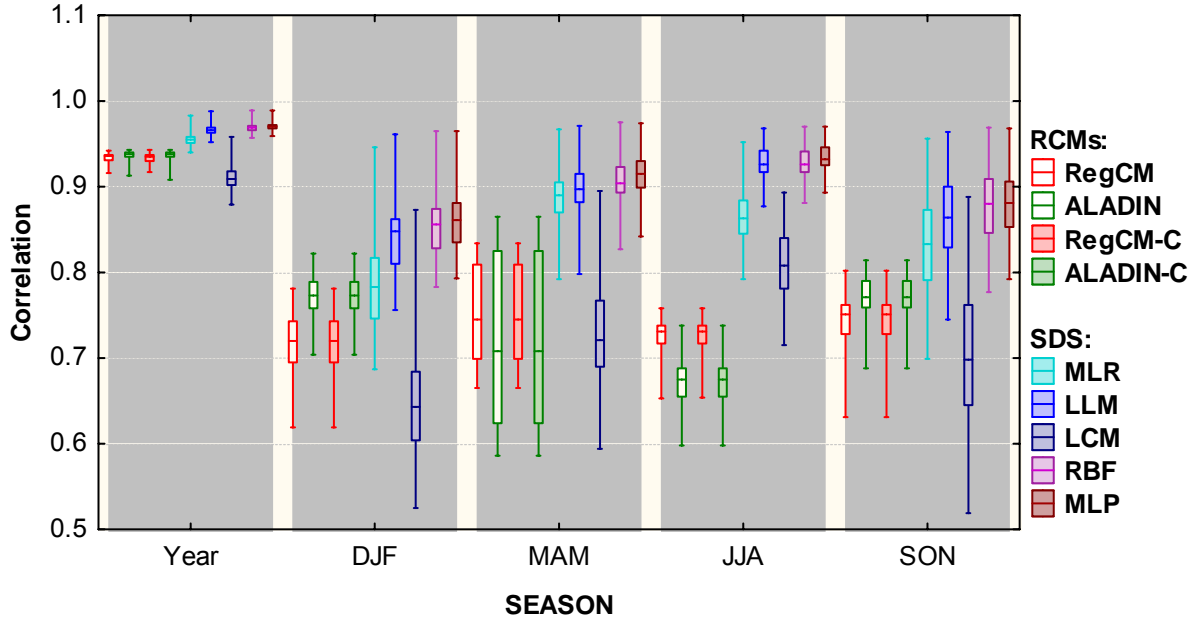
Fig. 2.8: Same as fig. 2.4, for **correlation of downscaled and observed mean daily temperature**.
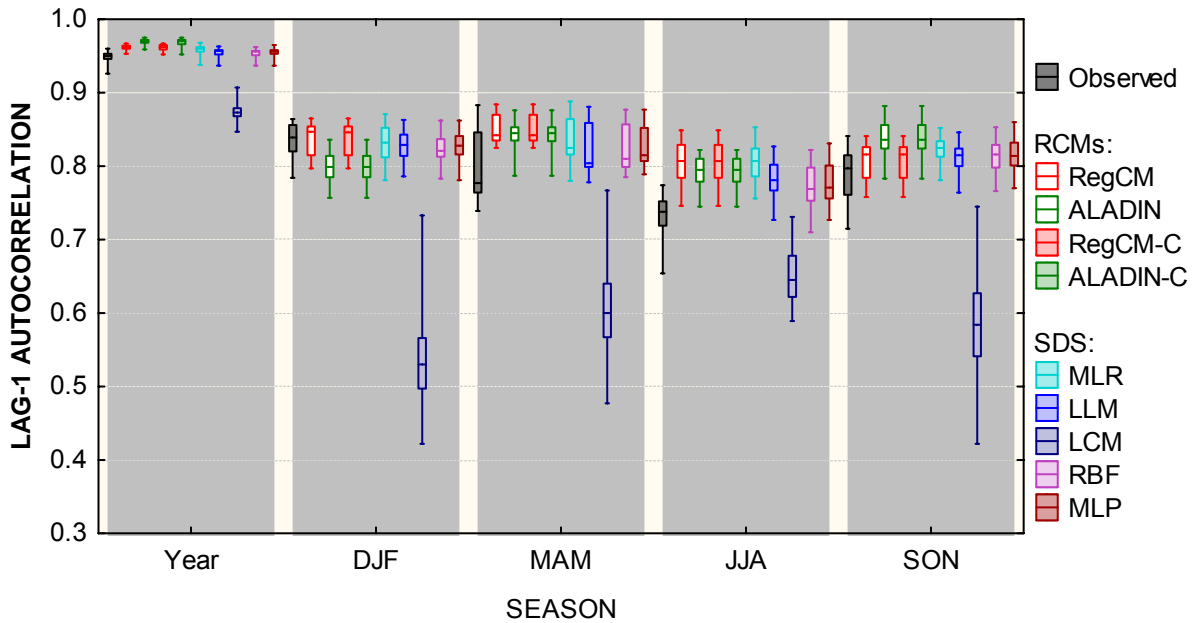
Fig. 2.9: Same as fig. 2.4, for **lag-1 autocorrelation of mean daily temperature**.

2.7.2 Daily maximum temperature

The results for daily maximum temperature are qualitatively similar to those for mean temperature. The systematic cold bias is still present for all methods in spring, as it is for both RCMs in summer at most stations (fig. 2.10). In winter, a warm bias is typical for all SD methods. The general tendency for lower dispersion of downscaled temperature is detected for both RCM, less so for the SD techniques (fig. 2.11), except for the LCM method, which typically produces series with rather higher-than-real standard deviation for individual months. The highest correlation and lowest RMSE are

11

usually found for the SD methods except for LCM (figs. 2.12 and 2.13), with RBF and MLP neural networks achieving the best fit between downscaled and observed data. A slight tendency for stronger persistence is still typical for all downscaling methods but LCM (fig. 2.14).
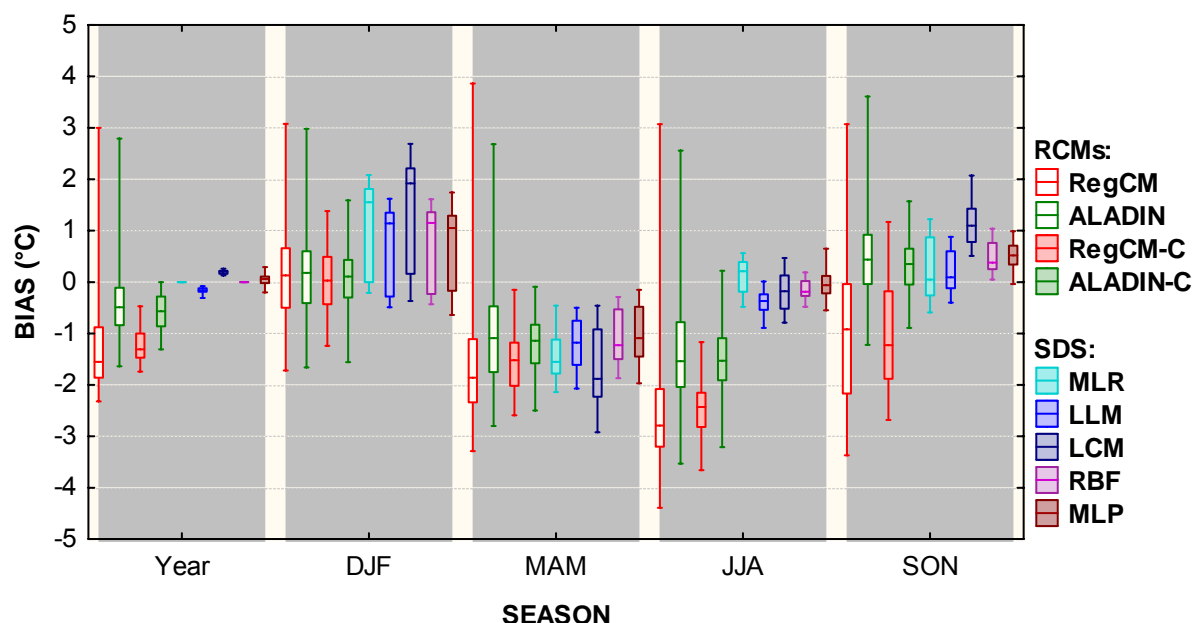
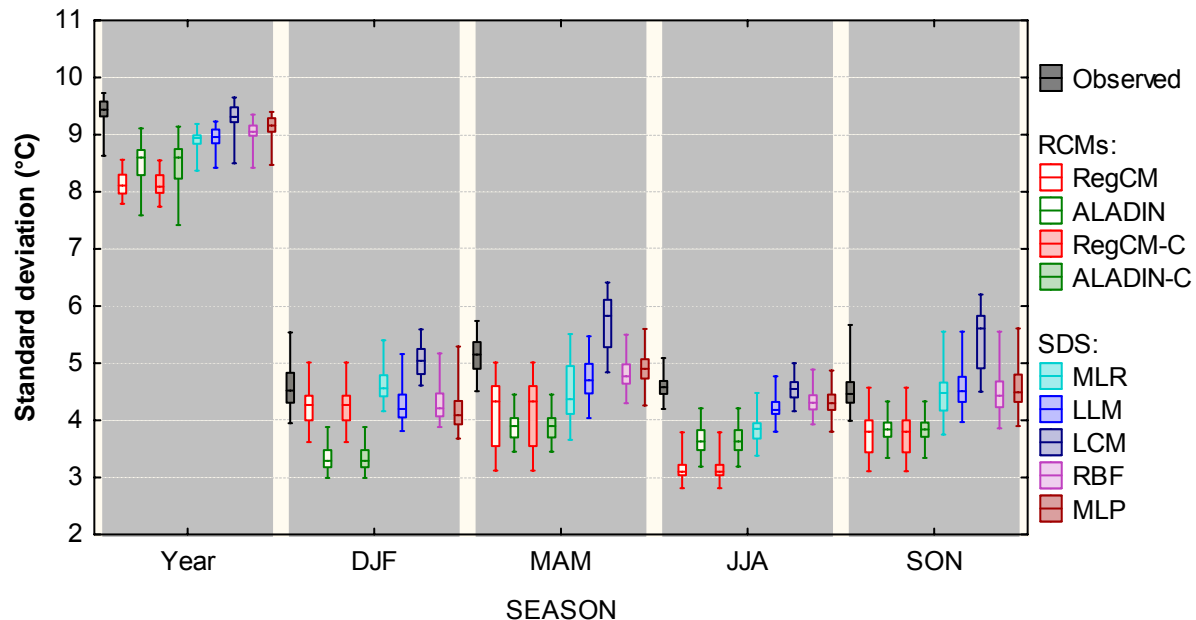**Fig. 2.10:** Same as fig. 2.4, for **bias of maximum daily temperature.**

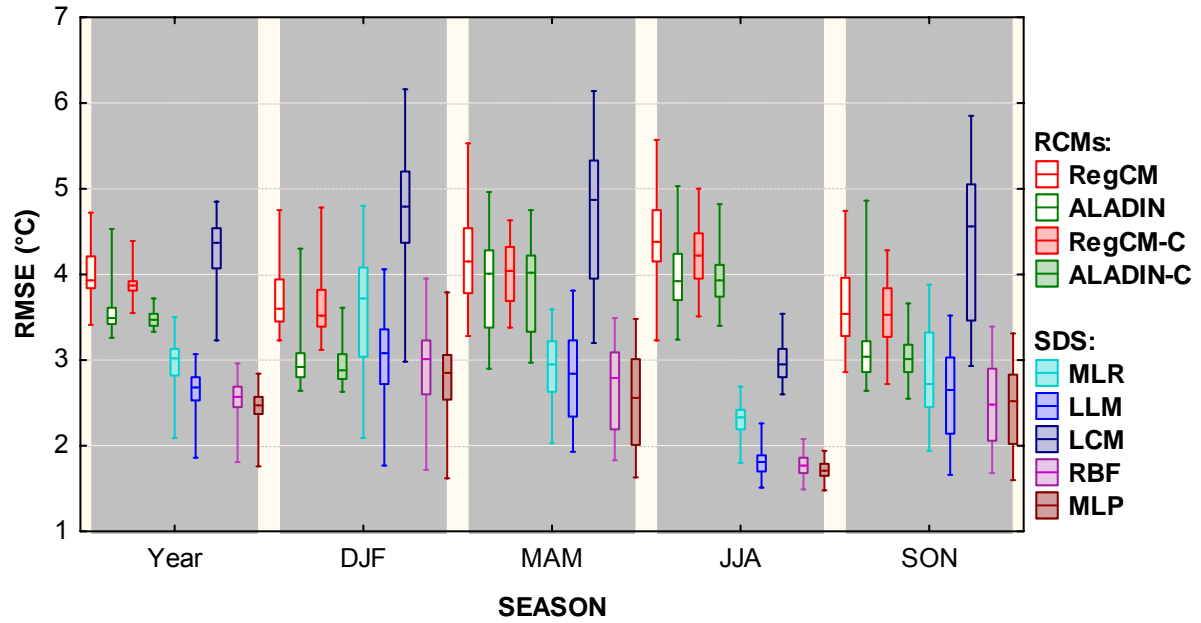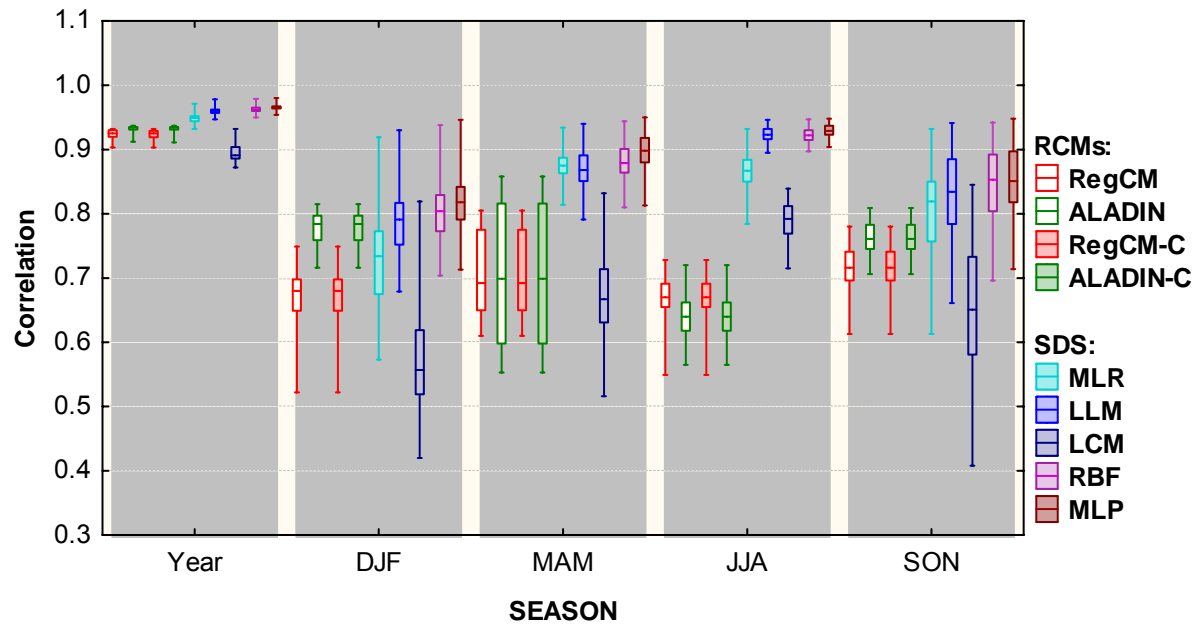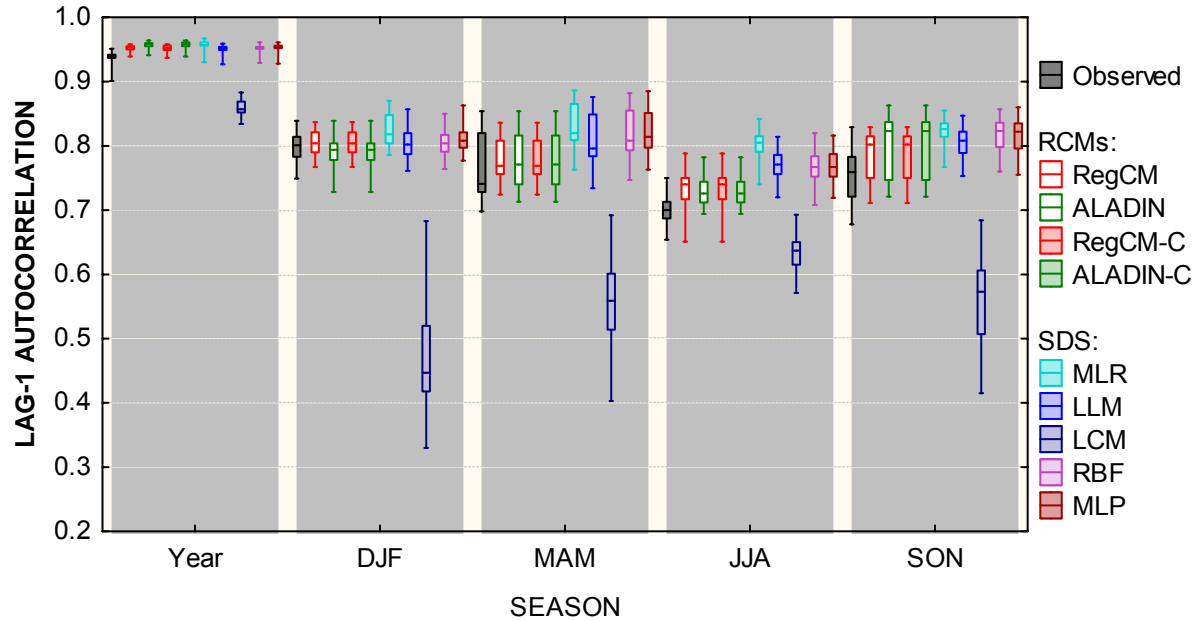**Fig. 2.11:** Same as fig. 2.4, for **standard deviation of maximum daily temperature.**

Fig. 2.12: Same as fig. 2.4, for **RMSE of maximum daily temperature** downscaling.

Fig. 2.13: Same as fig. 2.4, for **correlation of downscaled and observed maximum daily temperature** data.

Fig. 2.14: Same as fig. 2.4, for **lag-1 autocorrelation of maximum daily temperature** data.

2.7.3 Daily minimum temperature

Similarly to daily mean and maximum temperature, cold bias is typical for all methods of downscaling daily minimum temperature in spring (fig. 2.15), and for the RegCM model in summer. The underestimation of the series' dispersion is strongest for the ALADIN model, especially during winter months (fig. 2.16). The highest values of correlation and lowest RMSE are again typical for the SD methods except for LCM (figs. 2.17 and 2.18). A tendency for stronger persistence is still found for all downscaling methods but LCM (fig. 2.19), with the best match in winter (except for ALADIN, which somewhat underestimates autocorrelation in winter months).
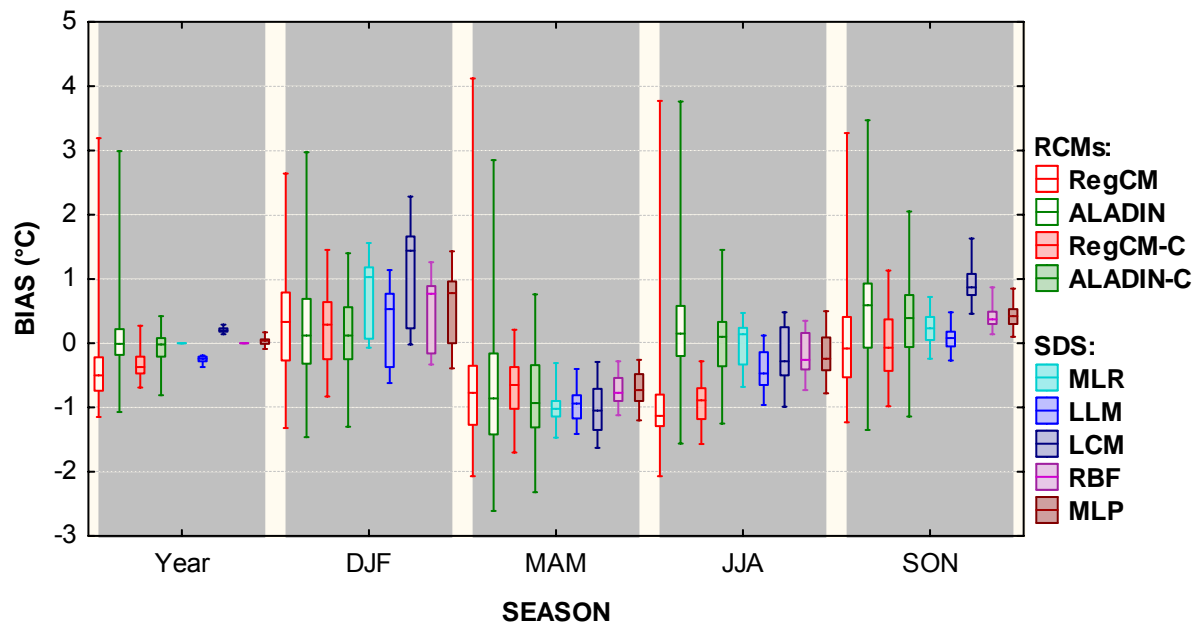

Fig. 2.15: Same as fig. 2.4, for **bias of minimum daily temperature.**
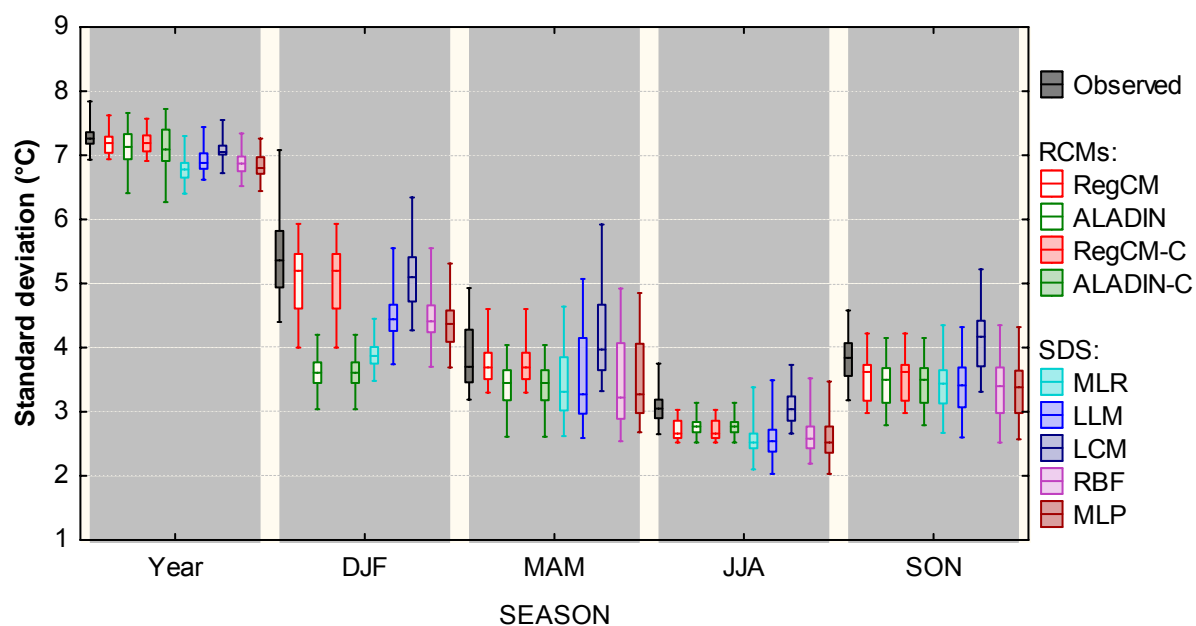
14

Fig. 2.16: Same as fig. 2.4, for **standard deviation of daily minimum temperature.**
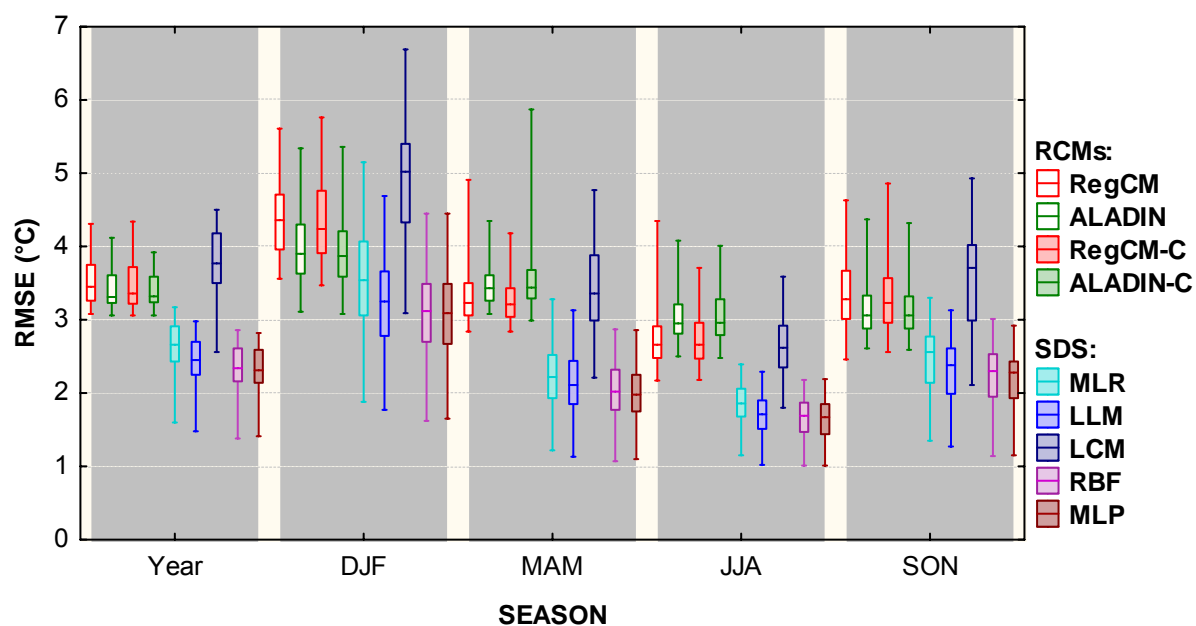

Fig. 2.17: Same as fig. 2.4, for **RMSE of daily minimum temperature** downscaling.
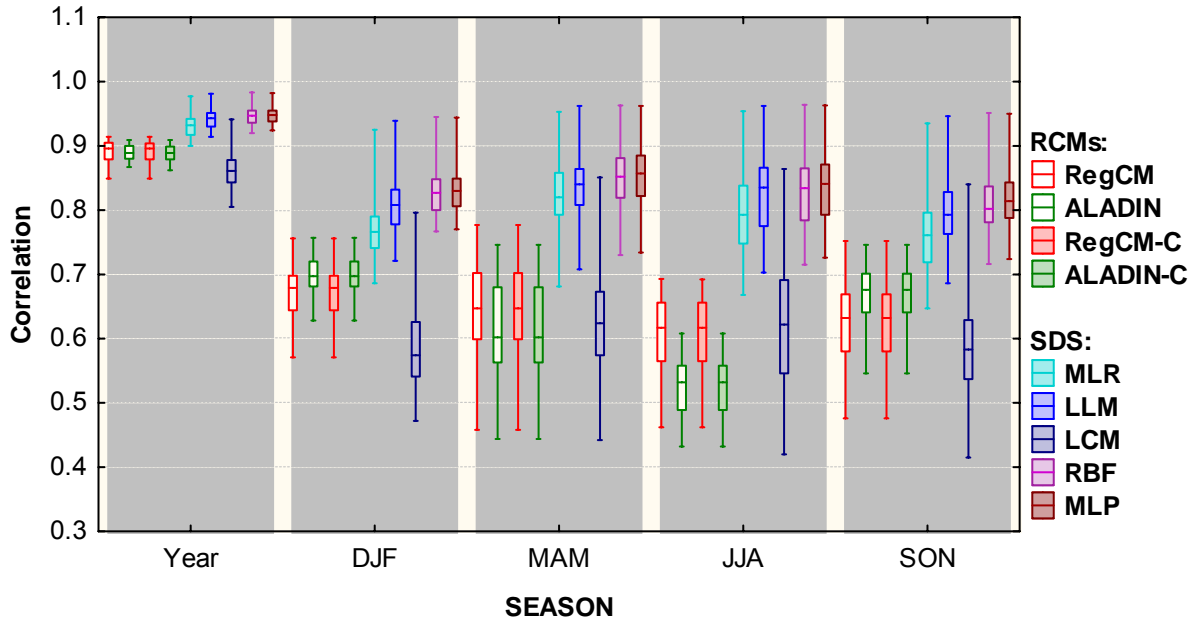
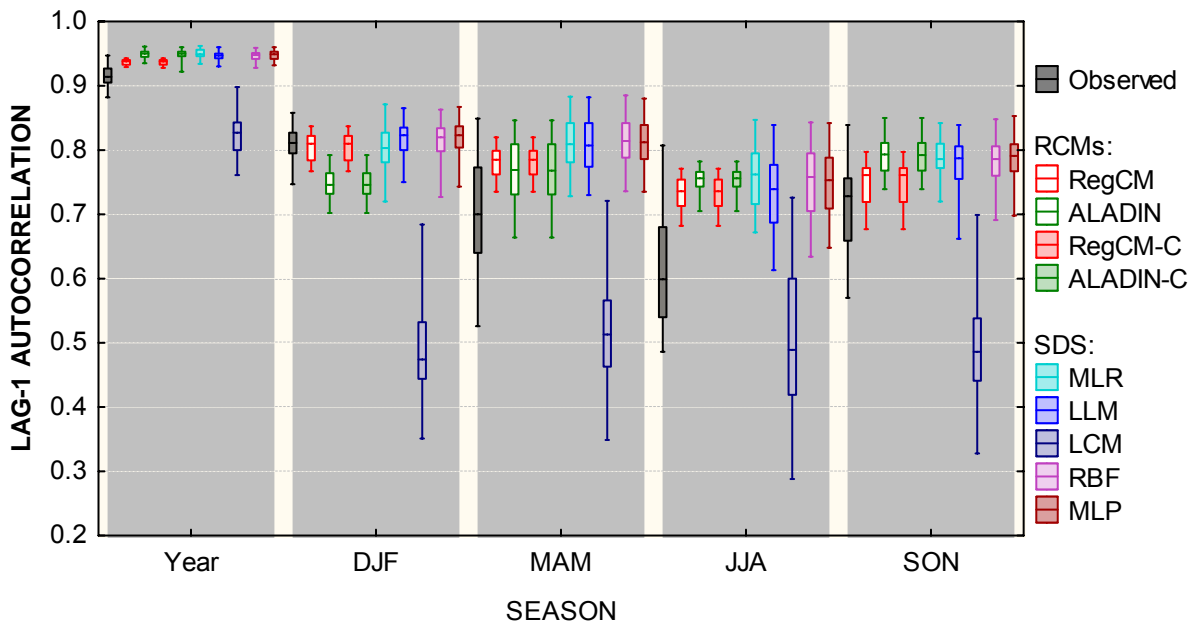**Fig. 2.18:** Same as fig. 2.4, for **correlation of downscaled and observed daily minimum temperature** data.

Fig. 2.19: Same as fig. 2.4, for **lag-1 autocorrelation of daily minimum temperature** data.

2.7.4 Daily precipitation

Monthly mean sums of precipitation are captured reasonably well by all methods but the RegCM model, which exhibits a strong wet bias throughout the year (fig. 2.20). Again, the exact value of bias varies with location of the station as well as month/season of the year, but the shape of the annual cycle of precipitation is captured realistically (fig. 2.26).

The deterministic connection between observed and downscaled data is rather weak for all methods. The relatively lowest values of RMSE (and highest correlations) were detected for the SD methods except for LCM, especially for both types of neural networks (figs. 2.22 and 2.23). Curiously, despite the wet bias of RegCM, the values of RMSE are almost identical for both regional climate models, probably because of the dominant influence of the misplaced days with high precipitation (as fig. 2.29 illustrates). It seems that no downscaling technique is able to reliably reproduce the location of precipitation events in time together with their magnitude, as scatterplots in fig. 2.28 show for four selected methods.

As for the statistical distribution of downscaled daily precipitation, the best fit is achieved by the LCM method (fig. 2.25). This, however, is due to the fact that LCM basically resamples the values of predictand from the training section of data. All other SD techniques show an extreme tendency to produce an overly symmetric distribution of values with lower than observed variance, underestimating the occurrence of both low and high precipitation amounts (as seen in fig. 2.27 for MLP), and strongly underestimating the number of days without precipitation. The ALADIN model reproduces the observed distribution of daily precipitation fairly well in autumn and winter, slightly less so in spring and summer (fig. 2.25). For RegCM, the statistical distribution is distorted by the wet bias. Also, the amount of days with precipitation < 0.1 mm is much smaller than in reality (fig. 2.27) for this model.

All SD methods but LCM produce precipitation series with too strong autocorrelation (fig. 2.24). This is consistent with their inability to respect the statistical distribution of observed precipitation, and cumulation of the precipitation amounts close to the mean value of the respective series. For RCMs (especially ALADIN), the persistence is more realistic.
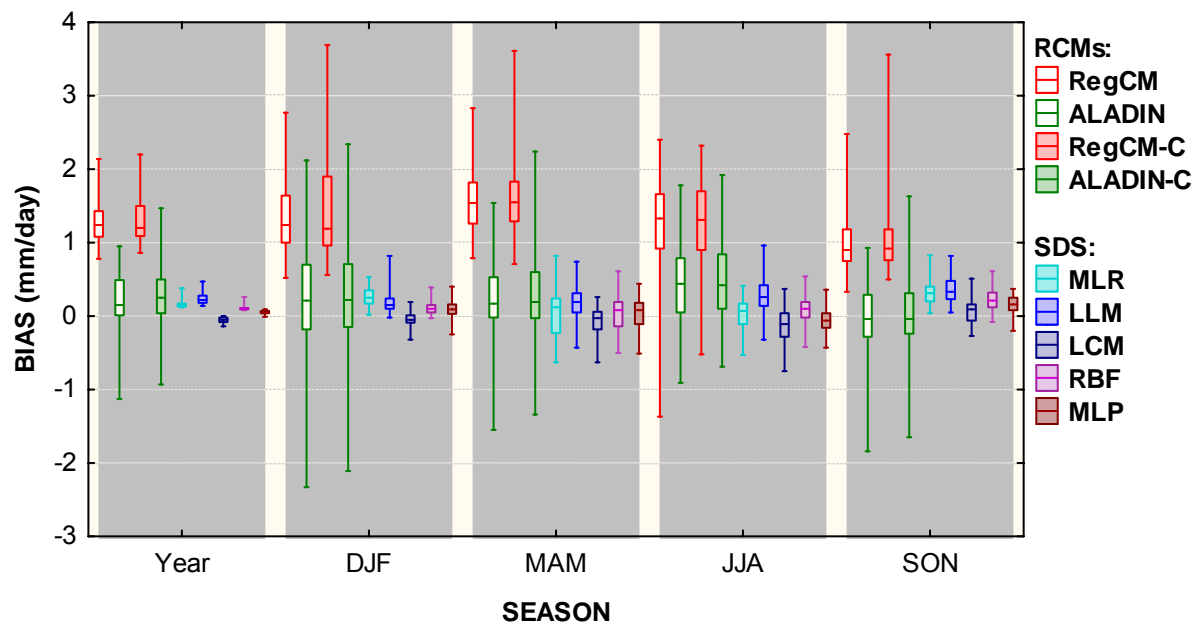
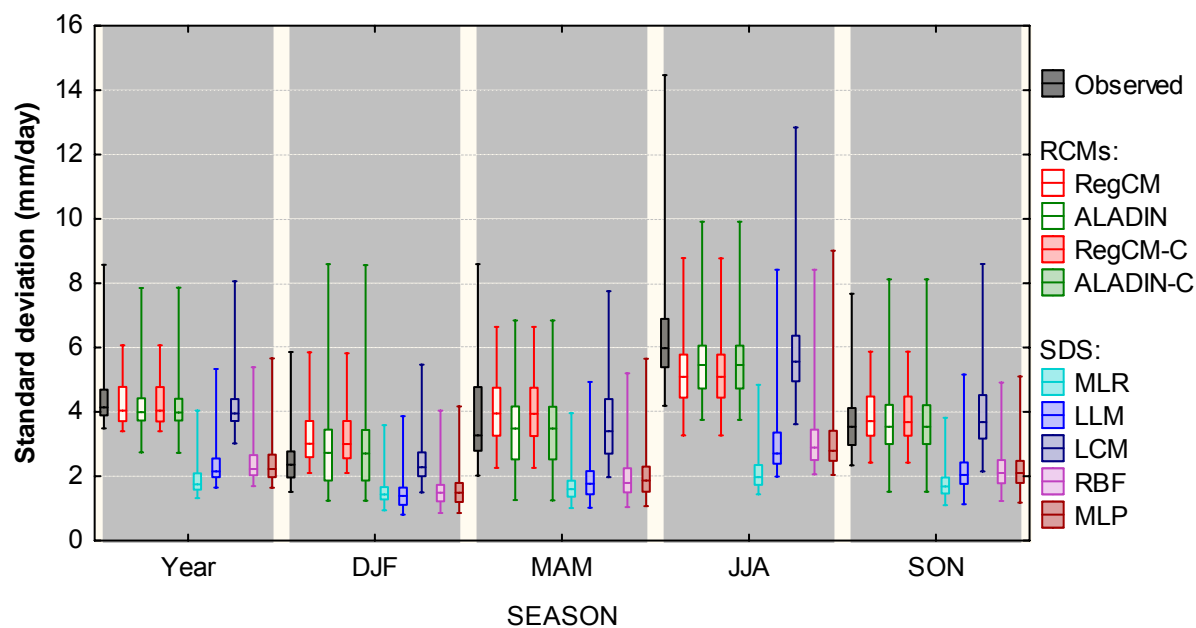**Fig. 2.20:** Same as fig. 2.4, for **daily precipitation bias.**

Fig. 2.21: Same as fig. 2.4, for **standard deviation of daily precipitation.**
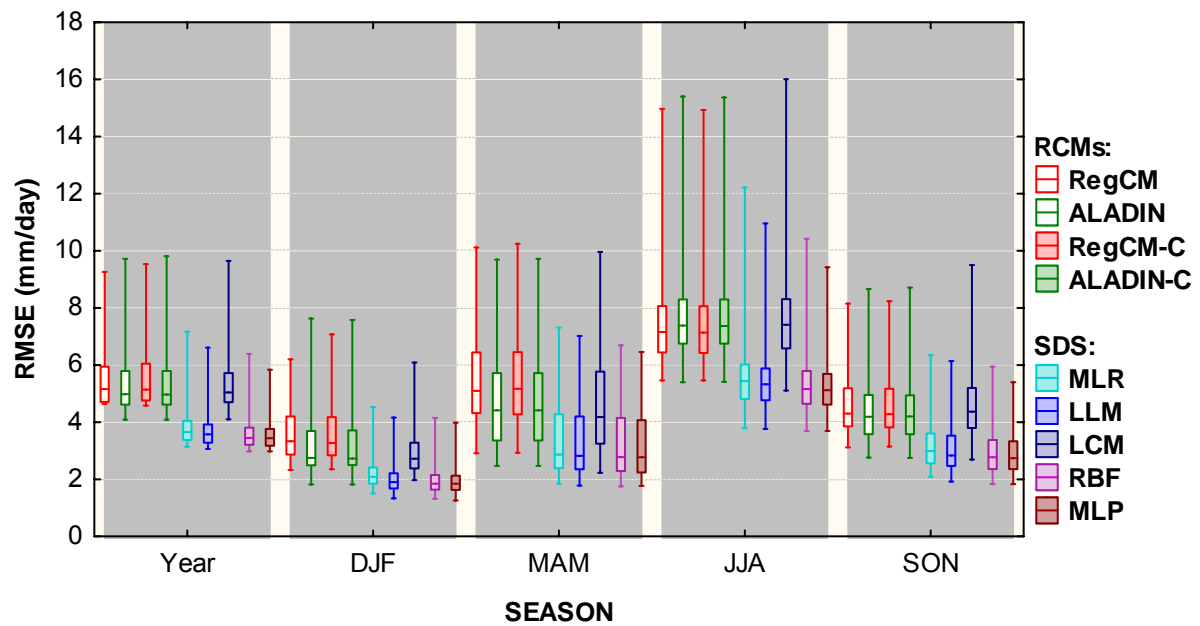
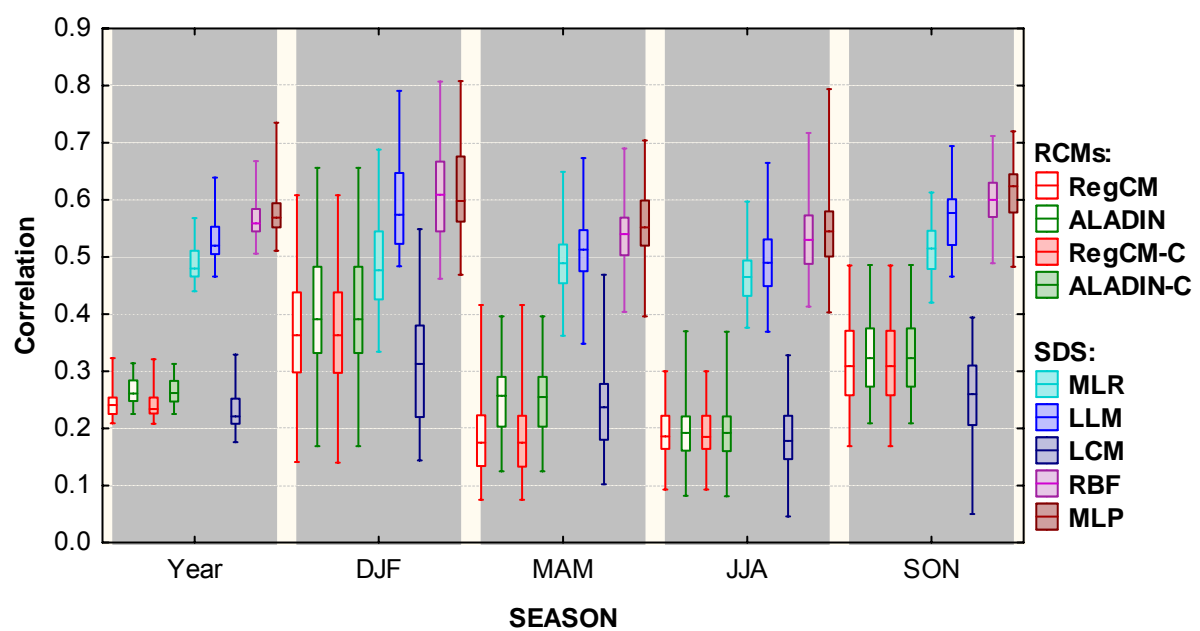**Fig. 2.22:** Same as fig. 2.4, for **RMSE of daily precipitation**.

Fig. 2.23: Same as fig. 2.4, for **correlation of downscaled and observed daily precipitation** data.
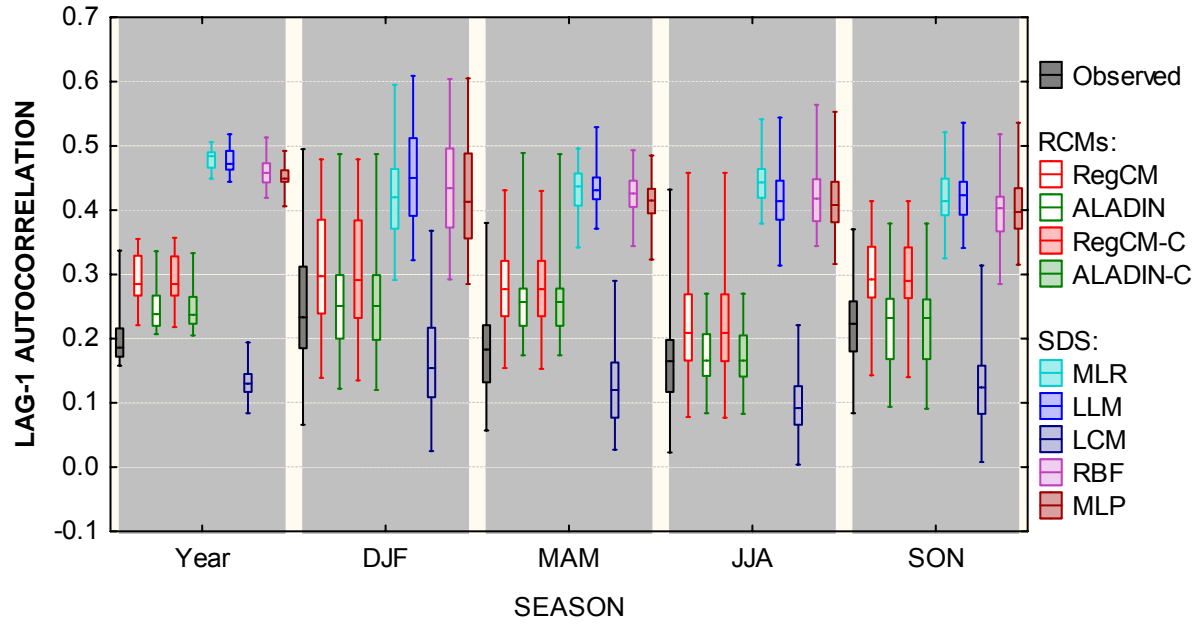
Fig. 2.24: Same as fig. 2.4, for **lag-1 autocorrelation of daily precipitation**.
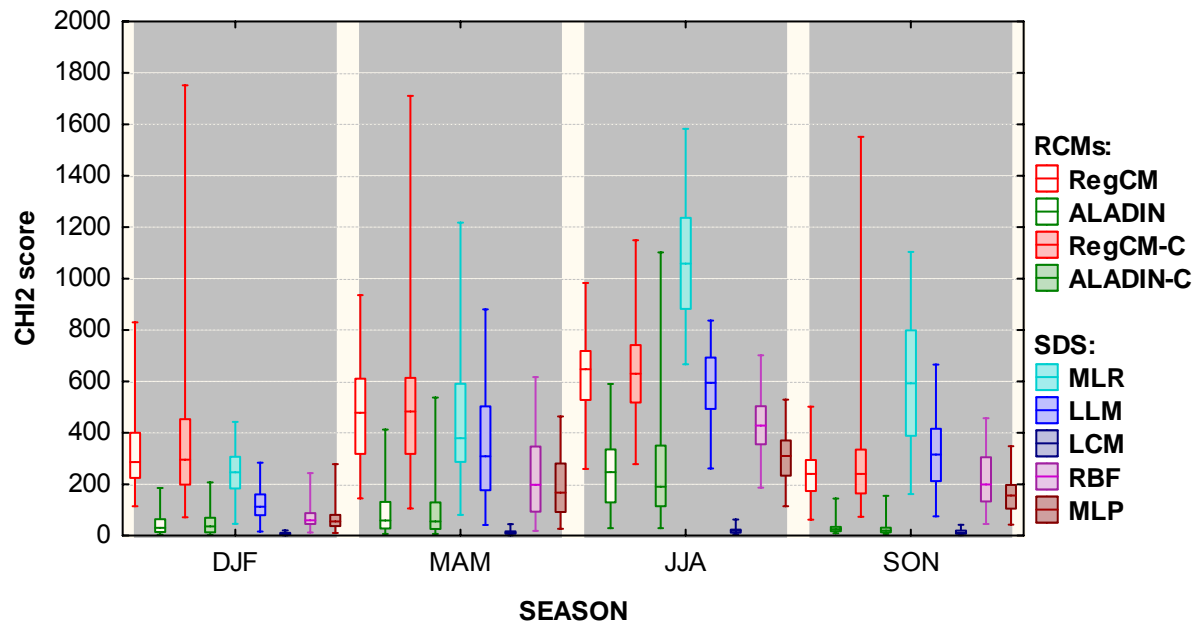
Fig. 2.25: Same as fig. 2.4, for **chi2 score** (as defined by eq. 2.1), derived from **daily precipitation** data.
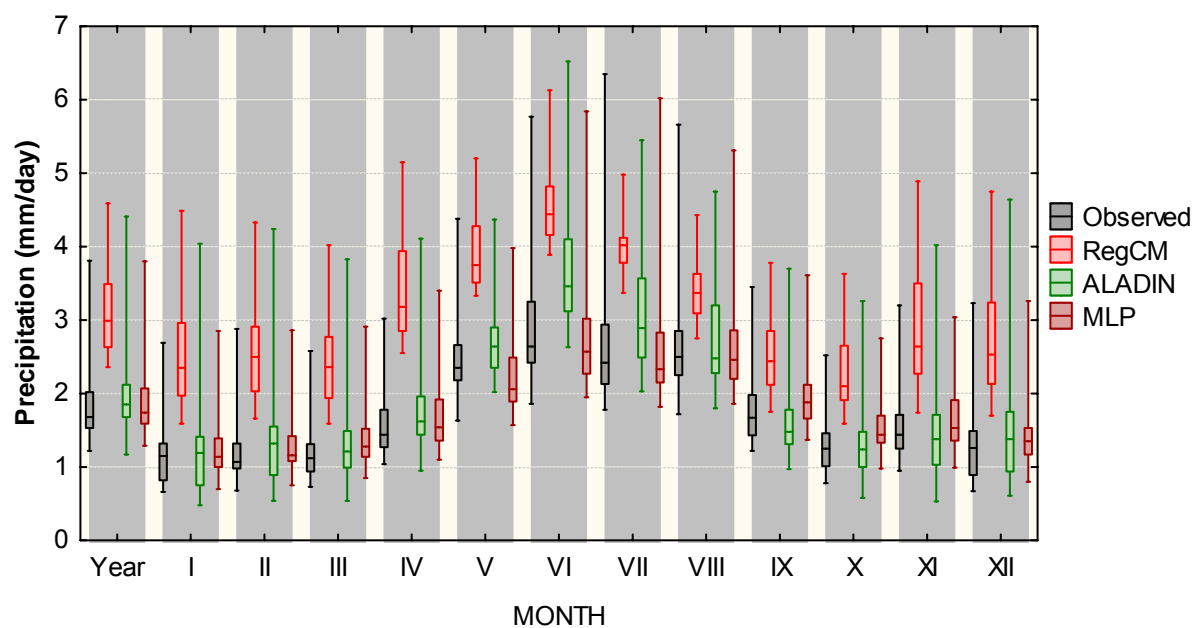
Fig. 2.26: Mean values of observed and downscaled precipitation, for the set of 25 Czech weather stations.

Fig. 2.27 Distribution of daily precipitation in January (upper panel) and July (lower panel), measured and downscaled by different methods (station Holešov).

Fig. 2.28: Plots of daily precipitation simulated by different methods of dynamical and statistical downscaling vs. observed precipitation (station Holešov).

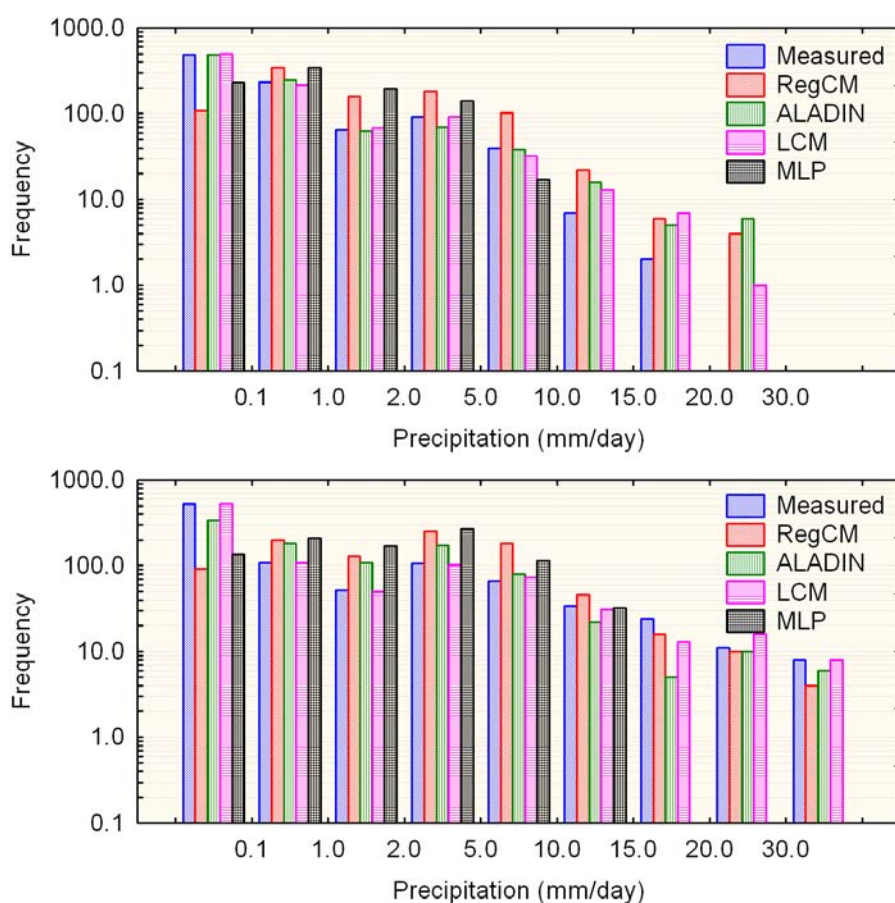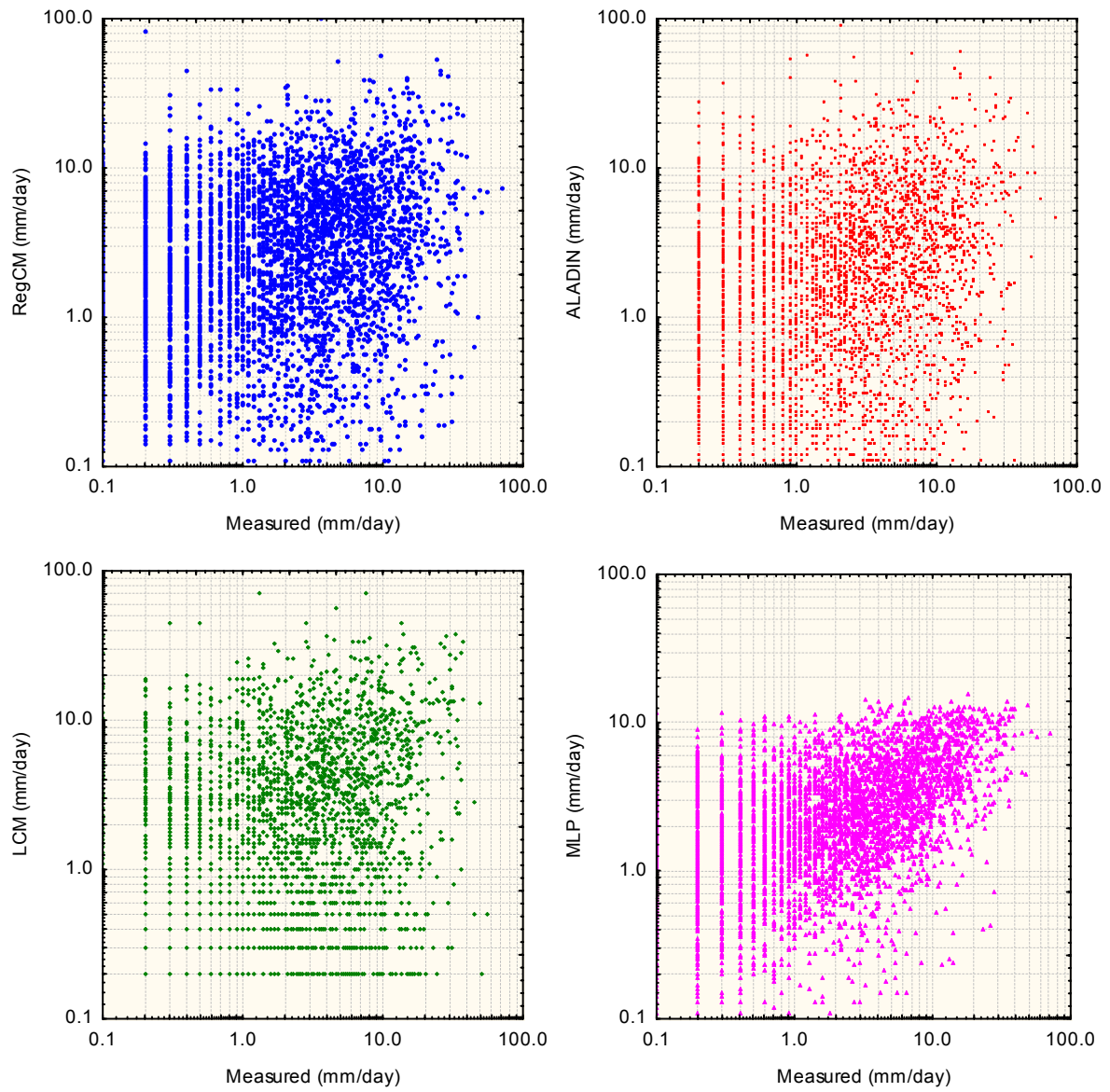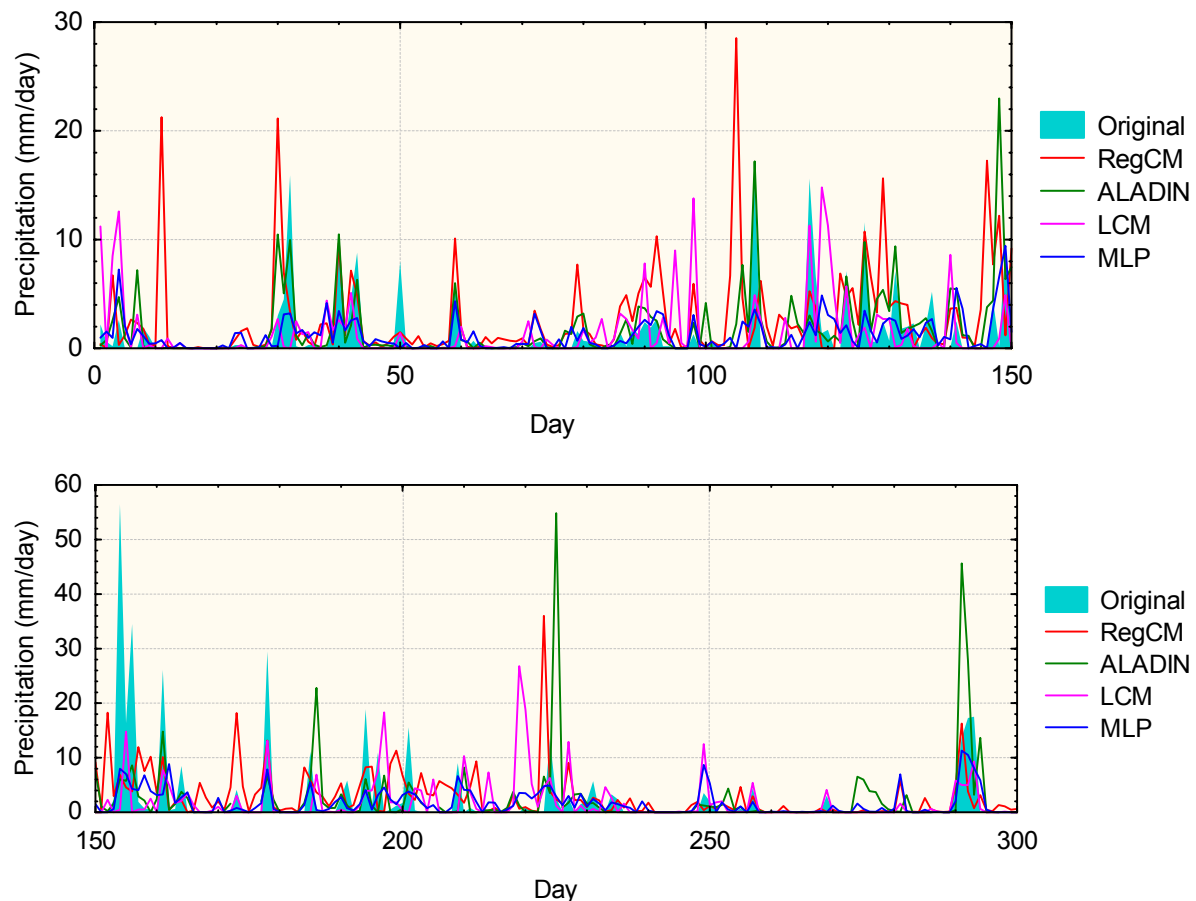**Fig. 2.29:** Time series of daily precipitation, observed and simulated by different methods of dynamical and statistical downscaling (station Holešov; the x-axis shows number of days since 1/1/1961).

2.7.6 Ranking of downscaling methods

Although it would be formally possible to sort the individual techniques according to any criterion, the above results indicate that such benchmarking would be of limited value, as the recommendation would vary with the type of variable as well as the season of the year. For the sake of consistency, it is beneficial to use the same downscaling method for all variables, and to select it according to the preferences of the follow-up impact-oriented application. Therefore, instead of a strict ranking, the basic conclusions have been summarized here:

- **For temperature data, no method seems to suffer from a critical, irremediable problem, with the exception of the LCM technique**. The high values of bias, detected in case of both regional climate models for some stations, are to the large part due to the altitude mismatch between the measuring site and the nearest grid point of the model. This can be easily amended by a correction computed from the vertical temperature gradient (such as eq. 2.2). Similarly, the eventual discrepancies of mean value and dispersion can be corrected by a simple linear transformation. Further bias-corrective techniques can also be used (deliverable D3.2). As for the SD techniques, there is no major difference between the character of outcomes of LLM, RBF and MLP methods. In most cases, they are superior to multiple linear regression (especially in terms of RMSE or correlation), although the gain is rather small on average. The LCM method does not seem to be suitable for downscaling of daily temperatures, because of the distorted temporal structure of its outputs (profoundly decreased values of autocorrelation).

23

- Precipitation downscaling is generally considered more challenging than downscaling of temperature, particularly for daily data, and none of the tested methods performed satisfactorily in all respects. The best match of the statistical distributions was achieved by LCM, which is working as a resampling technique, re-distributing values of predictand from the calibration set of data. On the other hand, only values already existing in the training set may appear in the downscaled series, making LCM unsuitable for situations when profound changes in the distribution of values are expected for the target variable in the future. LCM also tends to behave in a more stochastic fashion than other statistical methods, which causes a weaker correlation of its outcomes with the original series of measurements, and weaker autocorrelation within the downscaled series. The strong wet bias of RegCM (although partially correctable) indicates some serious problem of this model regarding precipitation. The nonlinear SD techniques (LLM, RBF, MLP) would require massive statistical corrections to be able to realistically reproduce daily precipitation series; the same goes for multiple linear regression. Therefore, without an intensive post-processing (such as a complete transformation of the shape of the statistical distribution of downscaled series), **the best choice for downscaling daily precipitation probably lies with the ALADIN model**, which produces series of daily precipitation with an autocorrelation structure close to observations, with a realistic enough distribution of values. In deliverable D3.2, it is demonstrated how the RCM outputs (both ALADIN and RegCM) can be further modified to eliminate not just most of the biases, but to bring a more realistic shape of the PDF in general to the simulated precipitation series.

The results presented above show a comparison done for the calibration/validation dataset of measurements obtained at Czech weather stations. Analogical analysis was also carried out for a gridded dataset of daily temperatures (maximum and minimum) and precipitation, created over the CECILIA Central-European validation domain (deliverable D3.1). Since the outcomes and conclusions are very similar to the ones presented above, they are not shown here; selected results were, however, included in the deliverable D3.2.

2.8 Temporal and spatial autocorrelations

Additional validation analyses were conducted on the common domain along the Czech/Austrain/Slovak/Hungarian borders; its more detailed description can be found in D3.1. Here we show an example for the ALADIN-Climate/CZ RCM nested in ERA-40 reanalysis. Two statistical properties, potentially important in various impact sectors, namely, spatial and temporal autocorrelations, are examined for daily maximum temperature (more precisely, for anomalies fro the mean annual cycle). The reality is represented by the gridded dataset, composed of observed data interpolated to the location of ALADIN's gridpoints – see Fig. 2.30.
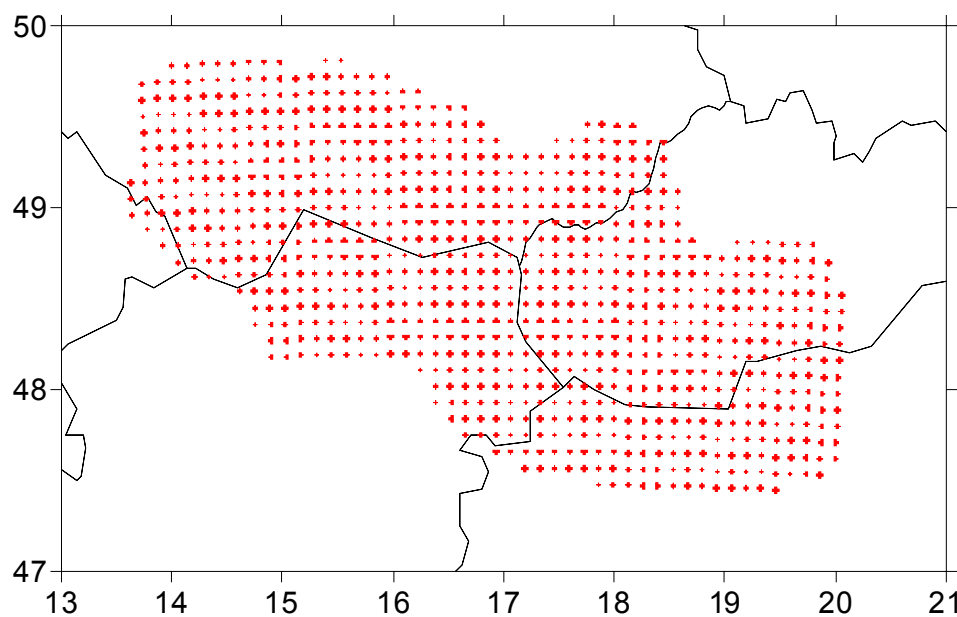
Fig. 2.30. Gridpoints used in the analysis.

24

PERSISTENCE, LAG 1 DAY
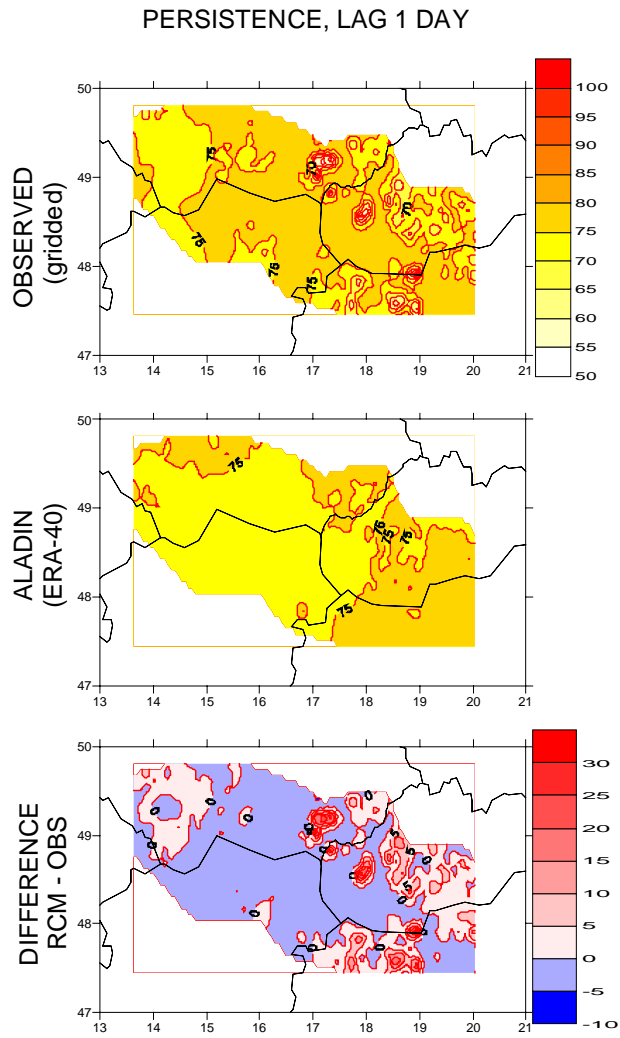
Fig. 2.31. Lag-1 autocorrelations (x100) in observed (gridded) data (top), RCM output
(middle), and their difference (model – observed, bottom).
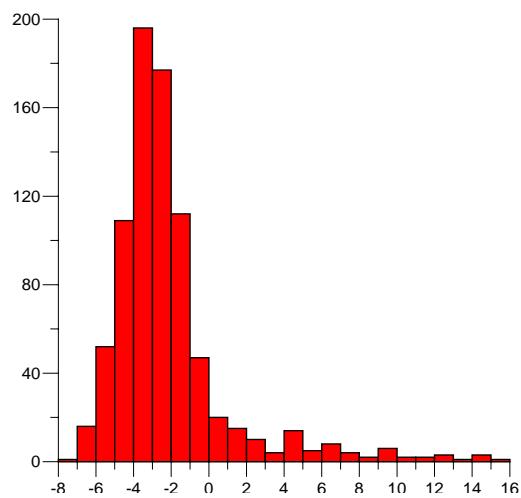
Fig. 2.32. Histogram of bias of lag-1 autocorrelations (x100).

SPATIAL AUTOCORRELATION
with 49.69N / 13.87 E

OBSERVED (gridded)

ALADIN (ERA-40)

DIFFERENCE RCM - OBS

Fig. 2.33. Spatial autocorrelations (x100) with the northernmost gridpoint (49.69°N, 13.87°E) in observed (gridded) data (top), RCM output (middle), and their difference (model – observed, bottom).

Fig. 2.34. Histogram of bias of lag-1 autocorrelations (x100).

The temporal autocorrelation, i.e, persistence, is expressed as autocorrelations with a lag of 1 day. Results are displayed in Fig. 2.31. Clearly, the persistence is lower in the RCM output (middle panel) than in observations (top panel) over a lar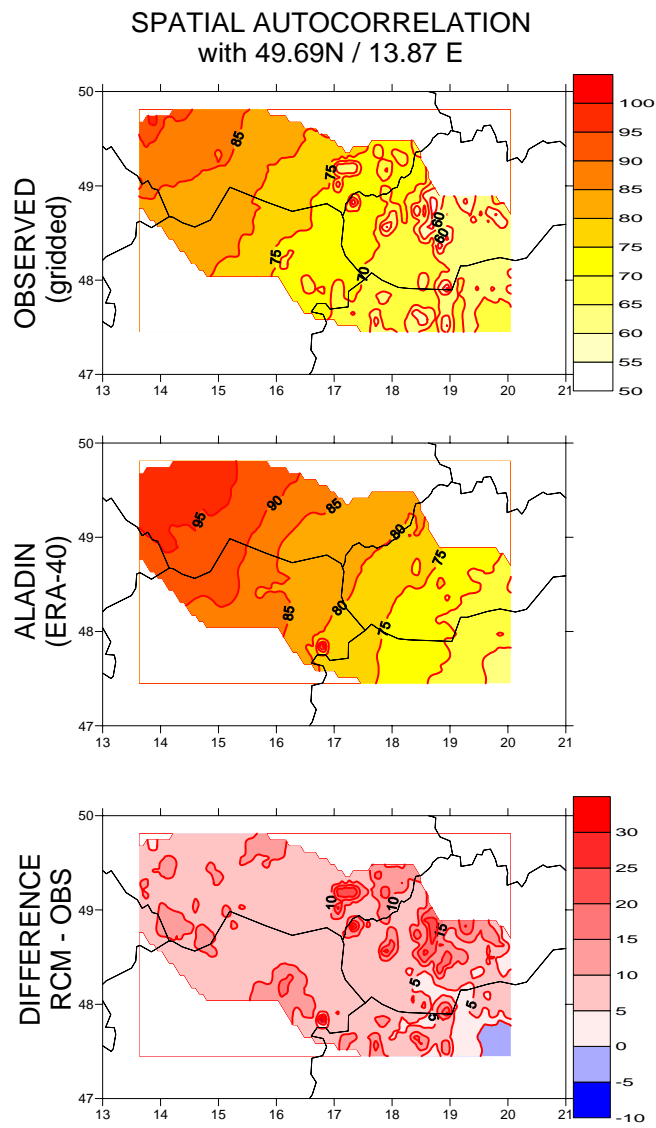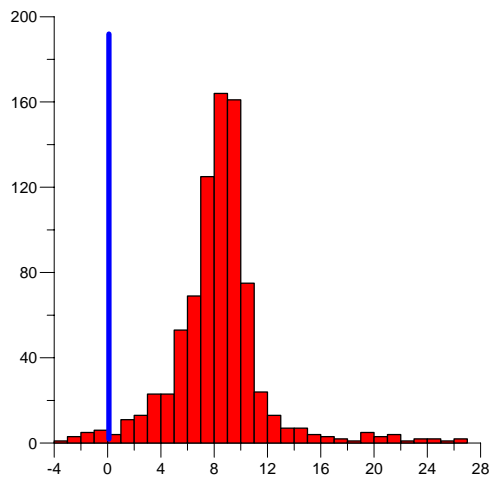ge part of the domain. Small scale features present in the map for observed data may be a result of orography or an artefact of the gridding procedure; however, they are of secondary importance since the differences (bottom panel) show a clear signal of an underestimation of persistence of between 0 and 0.05. An even clearer picture is obtained if a histogram of differences is produced (Fig. 2.32). The negative bias of persistence in the RCM output, peaking between –0.03 and –0.04, is obvious.

As an example of the spatial autocorrelation, we show autocorrelations with the northwesternmost gridpoint (49.69°N, 13.87°E) (Fig. 2.33). The decrease of autocorrelations is much less steep in the model than in reality, and this is especially so close to the reference gridpoint. That is, spatial autocorrelations are underestimated over the majority of the domain, with an exception of the most distant southeasternmost corner of the domain. Similarly to temporal autocorrelations, the positive bias of spatial autocorrelations can be well seen on the histogram of differences (Fig. 2.34). The mean as well as median of the bias of spatial autocorrelations amount to 0.083.

These results inform us that validation of RCM outputs should be conducted also for other quantities than mean and standard deviation.

References:

HMÚ (1972): Návod pro pozorovatele meteorologických stanic ČSSR, Hydrometeorologický ústav, Praha, 222 pp. (in Czech)

3. NMA contribution on the D3.3: Validation of the statistical downscaling models

3.1. Data and methods

The statistical downscaling models (SDMs) used by the NMA in the CECILIA project are based on the canonical correlation analysis (CCA) technique (Von Storch et al., 1993, Busuioc et al., 1999, 2006). These models have been developed for the mean temperature (94 stations covering the entire Romania) and precipitation total (16 stations covering a southeastern area, used for the impact studies in CECILIA). In a previous work (Busuioc et al., 2006) has been found that, in case of precipitation, it is difficult to find a single skilful SDM for the entire Romanian area, due to the complex Romanian topography. Figure 3.1 shows the position of the 16 stations used in this study. Compared to the previous studies, taking into consideration the impact needs, the SDMs have been constructed for monthly values.
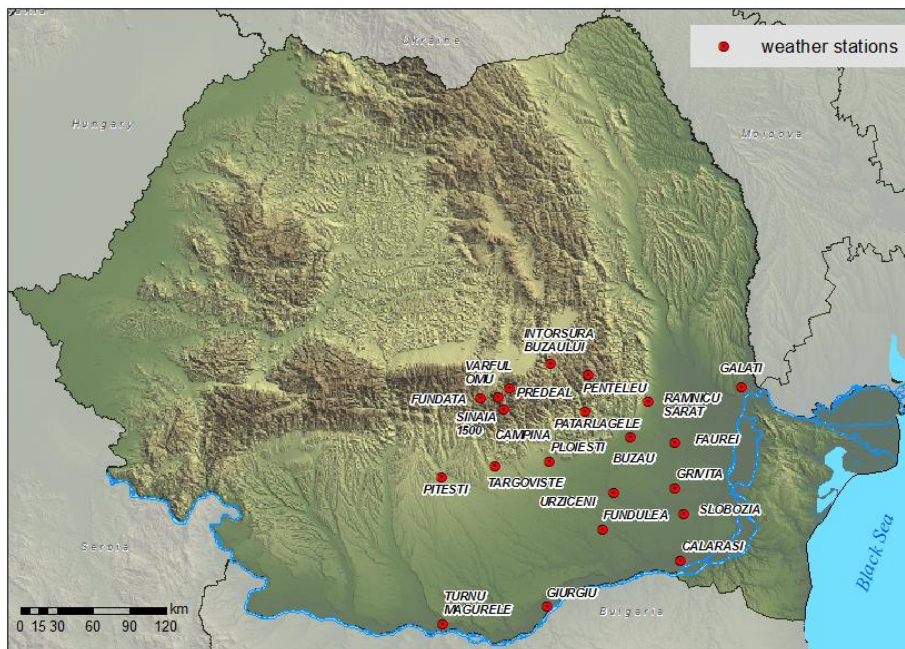
Figure 3.1. The location of the stations used in developing the SDMs for precipitation.

The temperature field at 850 mb (T850) has been considered as predictor for temperature while the sea level pressure (SLP), geopotential heights at 500 mb (H500) and specific humidity at 850 mb (separately or in combination) have been tested as predictors for precipitation. The predictor area and optimum predictor combination (number of EOFs used in CCA and number of CCAs used in SDM) has been selected so that the SDM skill (defined as correlation between observed and estimated values as well as fraction of the explained variance of estimated values from the total observed variance) is highest. The anomalies of the predictor and predictands projected onto the main EOFs (empirical orthogonal functions) have been used as inputs in the SDMs.

The temperature SDMs have been developed over the warm (May-October) and cold seasons, respectively, considering the respective monthly anomalies together. For precipitation, the SDMs have been developed for each of the four seasons (DJF, MMA, JJA, SON). In this

way, longer time series are available to calibrate and validate the SDMs, namely more 6 times for temperature and 3 times for precipitation. The stability of the skill, calculated over the independent data set, has been tasted, considering three validation intervals: 1961-1980 (fitting 1981-1999), 1981-1999 (fitting 1961-1980), 1991-2007 (fitting 1961-1990). The last validation interval has been considered in order to see if the SDM is capable to reproduce the extreme events during the last decades using the models calibrated over the 1961-1990. These models have been used to produce the scenarios for the near (2021-2050) and far (2070-2099) future. The predictors simulated through 9 GCMs (8 ENSEMBLES stream 1 simulations and ARPEGE) have been used as inputs in SDMs. The results are presented in the deliverables D 3.4 and D3.5.

3.2. Results
Temperature

It has been found that the optimum T850 area used as predictor in developing the SDM for monthly temperature anomalies at the 94 Romanian stations covers the area between 15E-35W and 35N-50N. For the warm season (May-October) a little bit higher skill is obtained for the area between 17.5E-32.5E and 40-50N. In figure 3.2, in case of the warm season, the SDM performance, represented by the explained variance, for two independent data sets (1961-1980, 1981-1999) is presented. It can be seen that the skill is high and stable, the highest values being for the western and intra-Carpathian area. Same spatial distribution of the skill has been identified for the cold season but with a little bit lower magnitude. In both cases the mountain stations present the highest skill, showing that the surface conditions are less important in these cases.
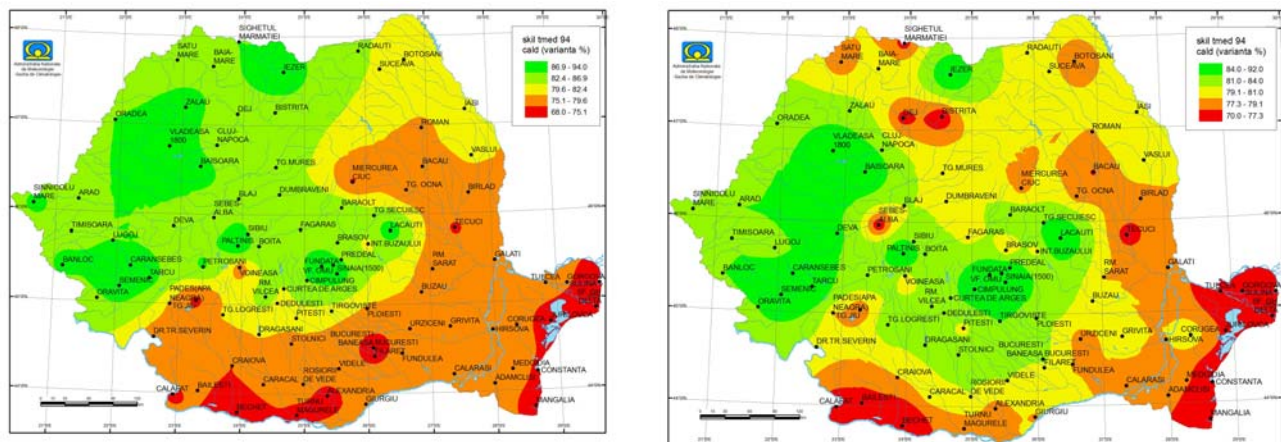
Figure 3.2. Skill of the statistical downscaling model, expressed as fraction of the explained variance by the estimated values from the total observed one, for the monthly mean temperature anomalies (May-October) derived for the two independent data sets (1961-1980, 1981-1999).

The SDM credibility in estimation the future temperature change have been tested by applying the SDM calibrated over the 1961-1990 to the T850 anomalies calculated over the period 1991-2007 against 1961-1990. It has been found that temporal evolution as well as the magnitude of the observed temperature anomalies is very well reproduced. Figure 3.3 shows an example for July.

Figure 3.3. Monthly temperature anomalies in July over the period 1991-2007 (against 1961-1990) calculated directly from observation (red) and indirectly from the T850 anomalies through the SDM calibrated over 1961-1990 (blue). Case of two stations: Turnu Magurele (SDM with the lowest skill-78% explained variance) and Sinaia (SDM with the highest skill-93% explained variance).

It can be seen that the strong anomalies from July 2007 are well reproduced but with a little bit lower magnitude, probable because of a persistent very dry soil conditions during the summer 2007.
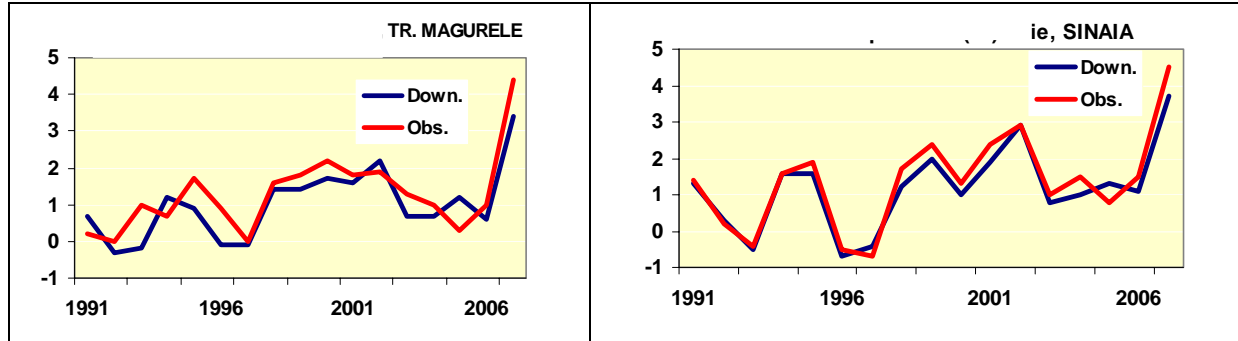
Precipitation

In case of precipitation, skilful SDMs have also been obtained, but the skill (even if it is significant at almost all stations) is lower. Since the explained variance is lower, the magnitude of the observed anomalies is not always well reproduced, compared with the temporal evolution which is better reproduced. Figure 3.4 shows an example for summer and winter.

Regarding the stability of the skill, there are differences between its magnitudes for different independent data set but the optimum combination of the predictors is placed among the models with highest skills. The obtained results show that the SLP is the best predictors for all seasons. In table 3.1 the SDM skill over the independent data set 1991-2007 with the model calibrated over the 1961-1990 is presented. It can be seen that the highest skill has been obtained for winter and lowest for summer. The SDM credibility in estimation of the future monthly precipitation change has been tested by applying the SDM calibrated over the 1961-1990 to the SLP anomalies calculated over the period 1991-2007 against 1961-1990. The observed and estimated changes are presented in Table 3.2. When the observed climate signal is strong and homogeneous over the entire analysed region (decrease during winter and increase during autumn), it is well reproduced by the SDM, showing that the precipitation variability over this region is well controlled by the large-scale SLP variability, this result being in agreement with previous studies (e.g. Busuioc and von Storch, 1996, Busuioc et al., 19999) when representative stations over the entire Romania have been considered. The not significant changes from summer and spring are also quit well reproduced. Considering the complex topography in the analysed region, these results are promising in order to obtain plausible future scenarios.

30

References

Busuioc A, von Storch H (1996) Changes in the winter precipitation in Romania and its relation to the large scale circulation. Tellus 48A: 538-552.

Busuioc A, von Storch H, Schnur R (1999) Verification of GCM generated regional seasonal precipitation for current climate and of statistical downscaling estimates under changing climate conditions. J Climate 12**:** 258-272 .

Busuioc, A, F. Giorgi, X. Bi and M. Ionita, 2006: Comparison of regional climate model and statistical downscaling simulations of different winter precipitation change scenarios over Romania. Theor. Appl. Climatol.,86, 101-124. von Storch H, Zorita E, Cubasch U (1993) Downscaling of global climate change estimates to regional scale: An application to Iberian rainfall in wintertime. J Climate 6: 1161-1171

von Storch H, Zorita E, Cubasch U (1993) Downscaling of global climate change estimates to regional scale: An application to Iberian rainfall in wintertime. J Climate 6: 1161-1171

Table 3.1. *SDM skill of the monthly precipitation anomalies at the 16 stations (Figure 3.1), expressed as correlation coefficient and fraction of the explained variance (*100), calculated for the independent data set 1991-2007 with the SDM fitted over the period 1961-1990. Negative values for the fraction of the explained variance indicate some events with opposite sign between observed and estimated anomalies*

Skill	Stations																
	1	2	3	4	5	6	7	8	9	10	11	12	13	14	15	16	M
Winter																	
Corelation	57	56	61	51	41	46	52	60	61	51	53	50	67	42	50	59	**54**
Variance	25	28	36	3	-1	13	26	32	31	25	26	21	38	-15	10	22	**20**
Spring																	
Corelation	36	51	63	45	56	38	51	47	38	55	53	58	38	41	36	63	**48**
Variance	13	23	37	19	30	15	25	21	14	30	27	33	14	13	12	34	**23**
Summer																	
Corelation	43	42	34	29	53	25	48	45	55	62	44	31	51	46	28	48	**43**
Variance	17	18	7	6	26	3	22	20	28	34	19	9	24	21	6	17	**17**
Autumn																	
Corelation	48	45	63	35	40	43	50	47	44	49	35	37	43	50	41	62	**46**
Variance	23	20	40	11	14	12	21	22	19	20	9	12	18	25	16	20	**19**

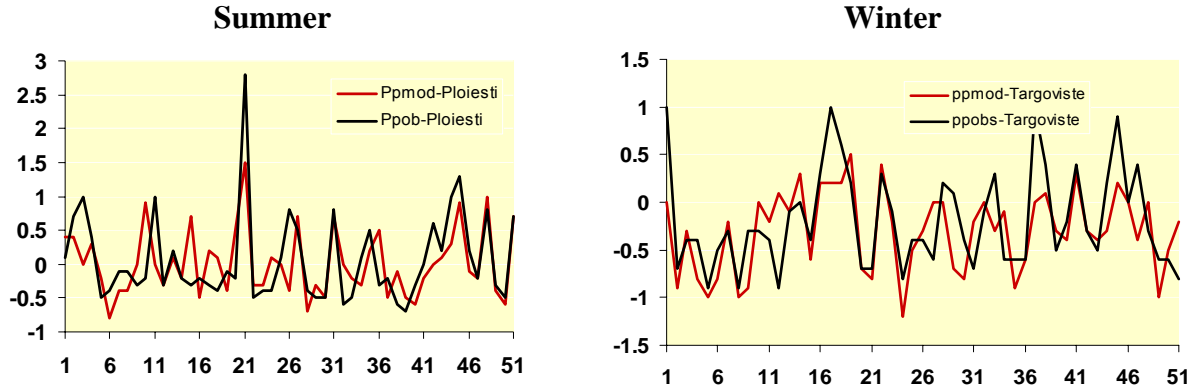*Figure 3.4. Standardised anomalies of the monthly precipitation for summer (Ploiesti station) and winter (Targoviste station) derived directly from observation (black) and indirectly from the SLP anomalies over the period 1991-2007 (against 1961-1990) through the SDM calibrated over the 1961-1990 interval. For every season the monthly anomalies are considered together. On the X axis their chronological order is noted.*

Table 3.2. *Change (%) of the monthly precipitation total over the period 1991-2007 against 1961-1990, derived directly from observations and indirectly through the SDM fitted over the period 1961-1990.*

	Station	XII		I		II		III		IV		V	
		Model	Obs.	Model	Obs.	Model	Obs.	Model	Obs.	Model	Obs.	Model	Obs.
1	Câmpina	-7.2	-2.5	-27.2	-23.1	-32.4	-49.1	6	-2.1	0.4	-6.6	-2.2	-23.5
2	Călăraşi	-18.7	14.2	-31.6	-1.9	-31.6	-27.7	7.8	34.7	-1.3	21.7	-4.4	26.6
3	Fundata	-16.7	1.8	-15.3	-17.1	-13.4	-8	14.5	51.2	0.9	-3.7	-2.2	-3.9
4	Fundulea	-12.6	-3.9	-33.5	-22.2	-36.3	-38.3	2.6	7.5	-3.7	3.4	-5.6	-5.4
5	Giurgiu	-10.5	7.1	-24.4	-19.6	-33.9	-8.4	19.1	5.2	7.5	-14.5	-2.7	-5.8
6	Griviţa Int.	-18.7	10.3	-36.9	-18.7	-35.6	-55.1	6.9	9.7	-3	11	-4.3	-19.4
7	Buzăului	-17.7	0.2	-14.6	-18.6	-13.6	10.8	23.7	41.3	1.7	8.5	-1.5	-13.8
8	Piteşti	-8.5	-10.7	-25.5	-5.4	-30.9	-20	11.5	15	3.2	10.8	-2.2	-3.5
9	Ploieşti	-11.2	9.5	-30.2	-9.7	-36.7	-33.5	6	11.2	-1	-8.9	-3.4	-18.1
10	Predeal	-12.3	-14.2	-15	-14.4	-15	-4.4	16.5	31.2	1.4	-10.5	-1.9	-8.7
11	Rm. Sărat	-9.5	22.6	-30.7	-13	-35.3	-39.7	12.8	12.5	3.2	-9.7	-2	-7.1
12	Sinaia	-2.2	0.7	-12.4	-20.8	-18.1	-23.9	6.3	1.1	-0.6	-19.4	-2.3	-19.2
13	Târgovişte Tr.	-8.4	-7.4	-24.3	-16.7	-31	-33.5	7.1	3.5	-0.1	-1.9	-3.3	-14.9
14	Măgurele	-9	-18.5	-21.2	-34.9	-29.9	-23.8	20.6	-15.1	8.6	-7	-3	1.4
15	Urziceni	-16.1	8.6	-35.3	-21.8	-34.8	-55	-2.5	-9.3	-7.1	-0.7	-6.3	-9
16	Vf. Omu	-26.1	-37.5	-23.8	-41.3	-23.7	-39	4.5	-16	-11.3	-32	-8.6	-33.1

	Station	VI		VII		VIII		IX		X		XI	
		Model	Obs.	Model	Obs.	Model	Obs.	Model	Obs.	Model	Obs.	Model	Obs.
1	Câmpina	-6.3	-2.7	4.1	4	11.5	19.7	29.7	48.5	8.7	0.1	14.2	0.1
2	Călăraşi	-12.3	-2.7	-11.5	-4.7	-0.4	0.7	22.9	70.6	6	32.6	3.6	32.6
3	Fundata	-10.2	-8.8	9.5	-6.7	12.3	11.4	27.2	26.5	18.2	9.8	8.1	9.8
4	Fundulea	-15.4	1.1	-3.7	32.6	6.4	8	22	48.5	3.5	86.2	1.2	86.2
5	Giurgiu	-14	3.4	-3.8	19.3	4.2	-8.5	25	40.8	7.8	72.4	2.1	72.4
6	Griviţa Int.	-11.8	21	-11.4	-6.5	0.3	-27.4	29.9	41.6	9.4	30.5	9.5	30.5
7	Buzăului	-10.4	0.3	-6.1	-11.1	1.9	20.9	23.9	16.9	16.2	14.1	7.9	14.1
8	Piteşti	-10.5	-14.7	11.8	21.8	19.8	36.1	32.1	46.1	11.6	19.1	15	19.1
9	Ploieşti	-5.9	-2.1	4	0.7	12.4	21	24	53.6	2.8	36.8	10.5	36.8
10	Predeal	-9	-9.5	-1.1	-8	5.7	22.4	25.6	26.3	20.3	8.8	8.4	8.8
11	Rm. Sărat	-11.5	-1.1	-6.9	10.1	2.2	17.9	26.9	21.2	9.9	68.5	12.5	68.5
12	Sinaia	-8.3	-8.4	9.2	-10.1	13	16.7	31.8	33.6	13.5	0.9	13.8	0.9
13	Târgovişte Tr.	-6.6	-5.8	8.8	0.5	17.6	40.1	33.2	52.4	9.8	28.1	14.3	28.1
14	Măgurele	-15.4	-15.9	0.9	8.5	5.2	4.9	28.7	56.4	5	39.4	6.9	39.4
15	Urziceni	-13.7	6.8	-7.3	19.4	3	-2.7	25.1	56.2	4.8	41	5.2	41
16	Vf. Omu	-12.5	-19.4	7.3	-13.1	8.5	-7.2	19.3	17	14.5	-8.7	-11.7	-8.7

4. Contribution by OMSZ: validation of ALADIN/Climate/HU

OMSZ in their contribution to D3.3 concentrated on a basic validation of the Hungarian version of the ALADIN RCM for the Hungarian territory.

4.1. Basic description of ALADIN-CLIMATE/HU

- Model version: ALADIN-Climate V4.5
- Domain: Carpathian Basin (lat: 44.64 – 50.01 N; lon: 12.44 – 25.22 E)
- Horizontal resolution: 10 km
- Integration period: 1958 – 2000
- Evaluation period: 1961 – 1990
- LBC: ERA-40; coupling: 6h
- Dynamics: Spectral model
  Hydrostatic
  Hybrid vertical coordinates
  SISL advection scheme
  LBC: Davies-scheme
  Prognostic variables: surface pressure
  temperature
  horizontal wind components
  specific humidity
- Physics: FMR radiation scheme
  ISBA scheme for soil
  Bougeault scheme for deep convection
  Ricard and Royer scheme for large scale cloudiness
  Smith scheme for large scale precipitation

4.2. Observed data for validation

- **CRU 10'** (**www.cru.uea.ac.uk**)
- **HUGRID:** Interpolated gridded dataset (0.1 deg regular grid) over Hungary

4.3. Validation

4.3.1. Annual temperature

Comparing the model simulation to CRU10' and HUGRID observations, generally speaking 1-3 degree underestimation had been found. The errors are higher in the Alps and near to the model boundaries.

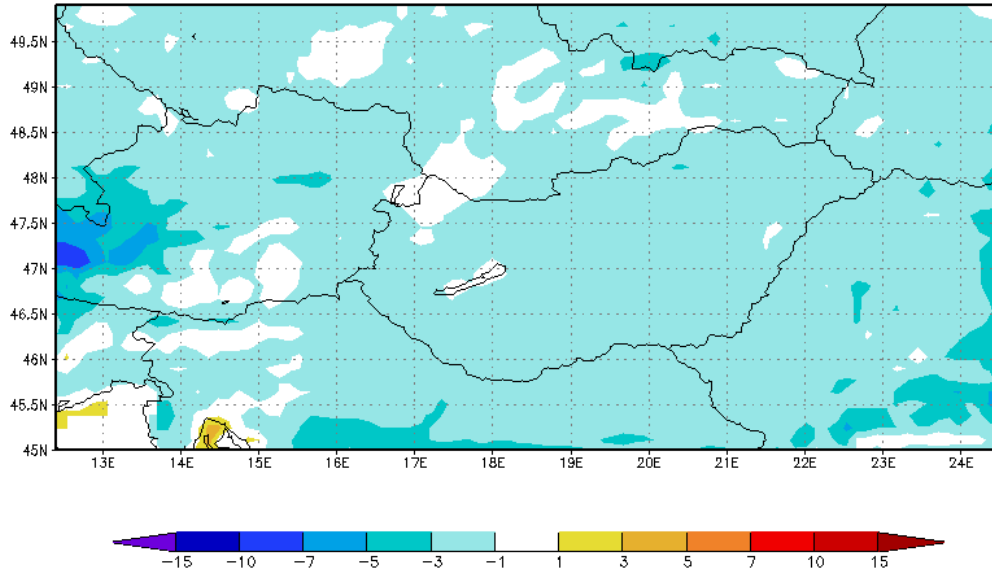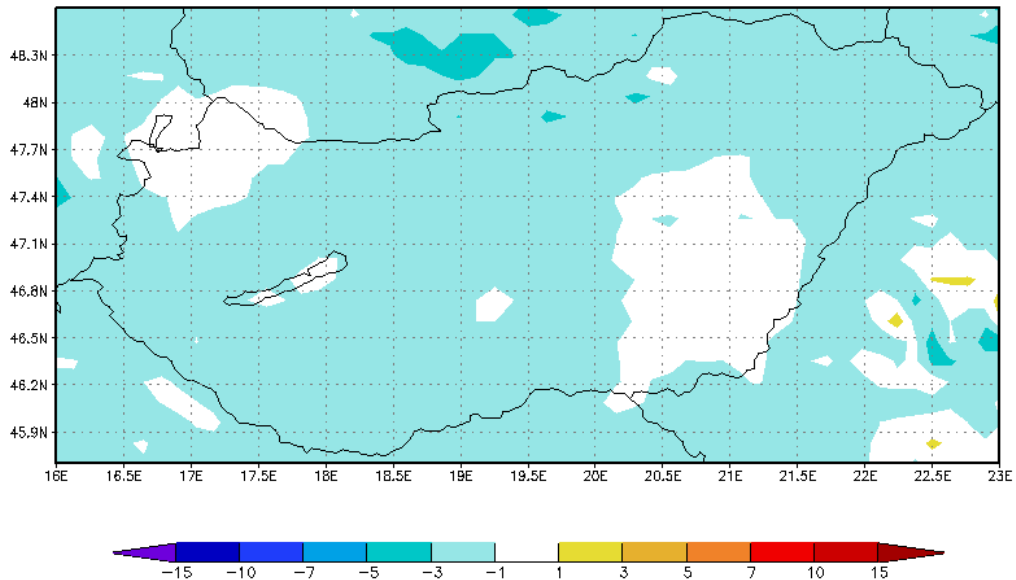*Fig. 4.1. Difference of annual mean temperature (ALADIN-CLIMATE – CRU(10')*
[ᵒC])

Fig. 4.2. Difference of annual mean temperature (ALADIN-CLIMATE – HUGRID
[ᵒC])

4.3.2. Seasonal temperature

Regarding the seasonal mean temperature, in spring and autumn a higher underestimation can be noticed than in the annual case. The errors generally exceed even the 5 degree in

some mountainous places, and even 7-10 degree in the Alps. In summer the model is quite perfect, in winter the simulation is colder than the observations, but this underestimation is not as large as in the transitional seasons.

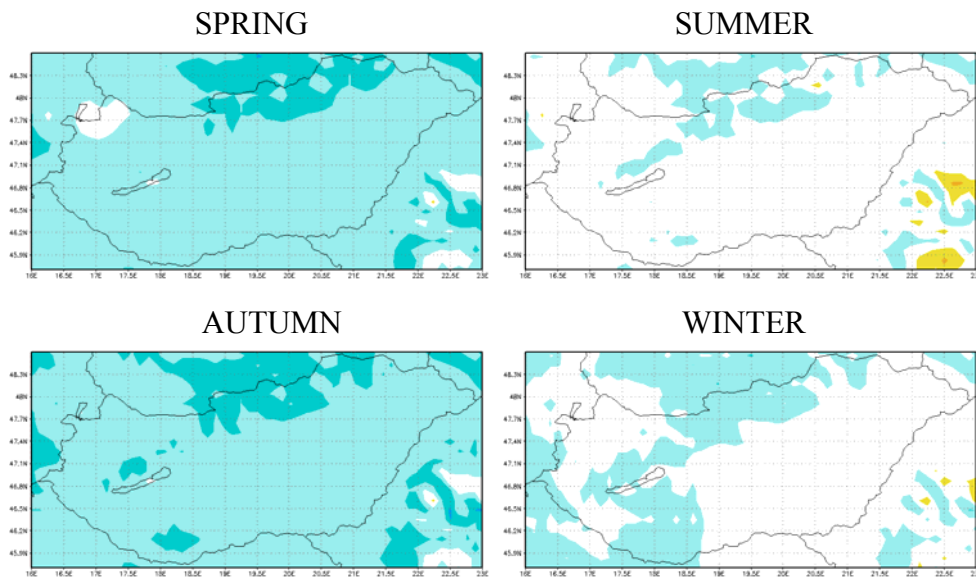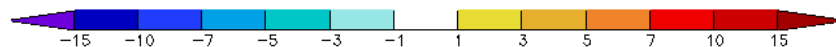***Fig. 4.3. Difference of seasonal mean temperature (ALADIN-CLIMATE – CRU(10')*** *[^{o}C])*

SPRING   SUMMER

AUTUMN   WINTER

Fig. 4.4. Difference of seasonal mean temperature (ALADIN-CLIMATE – HUGRID *[^{o}C])*

SPRING   SUMMER

AUTUMN   WINTER
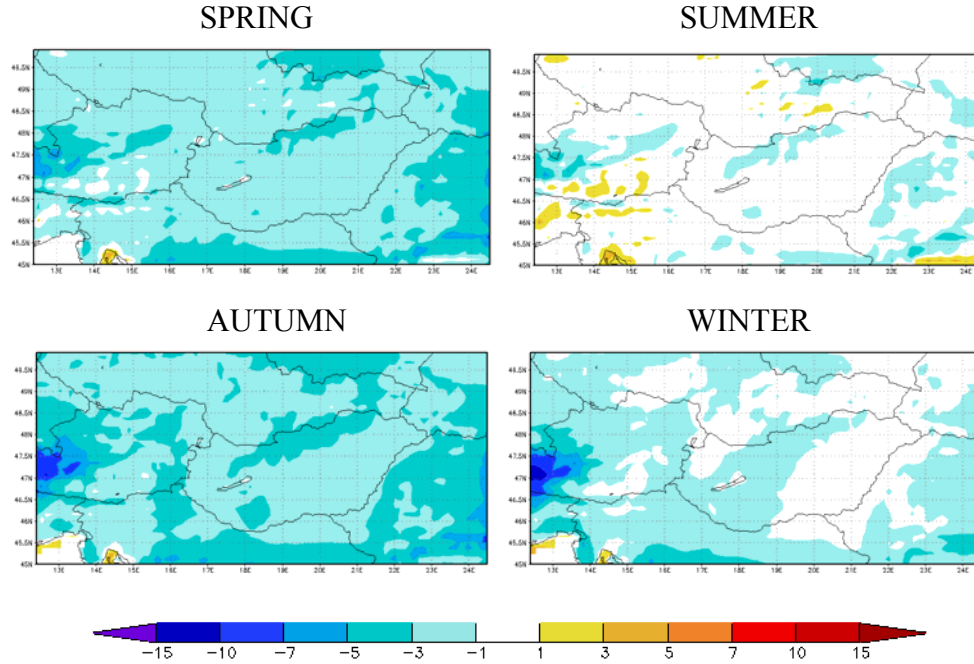
4.3.3. Annual precipitation

Looking at the annual relative difference of precipitation, the biggest errors can be noticed at the edge of the domain. Still, the relative difference remains moderate in the south-west part of the Carpathian Basin.

Fig. 4.5. Annual relative difference of precipitation
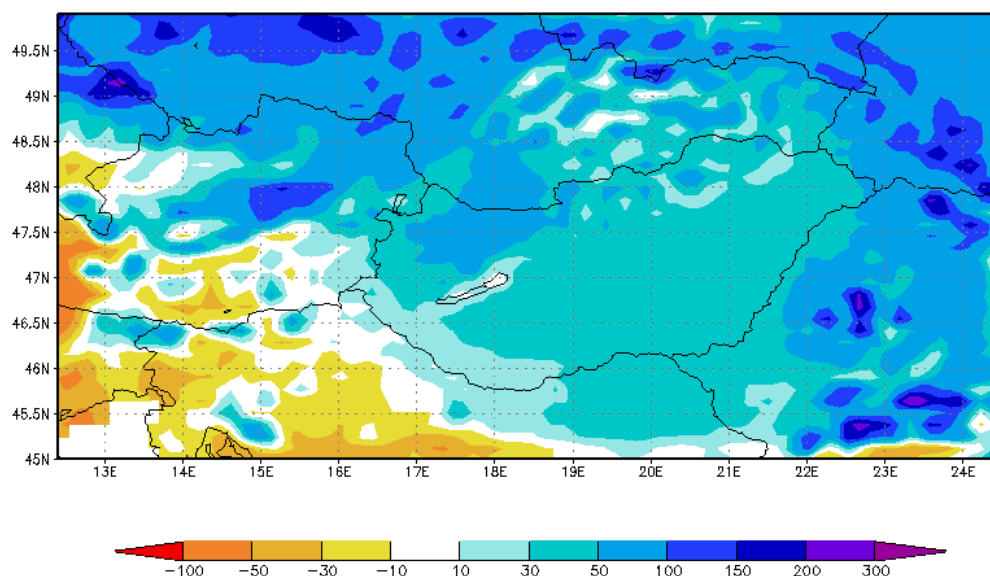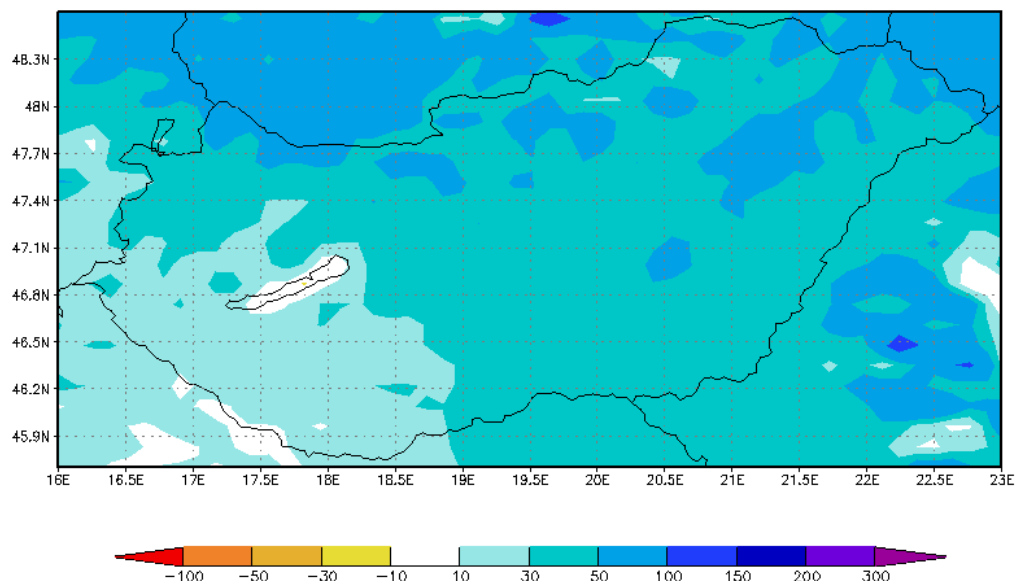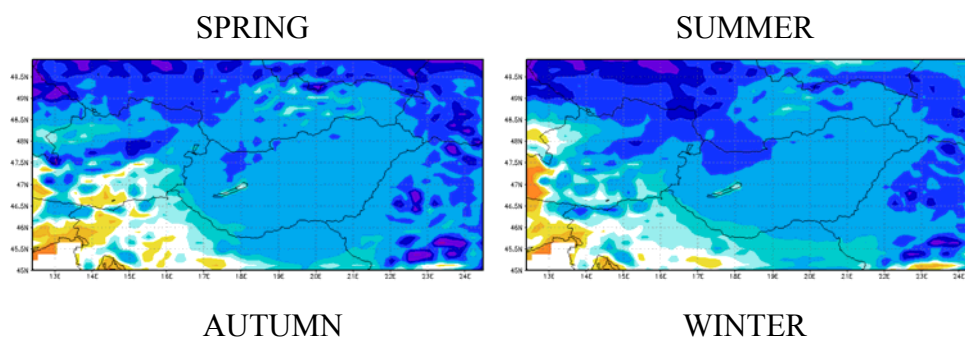*[ALADIN-CLIMATE – CRU(10')]/CRU(10') [%]*

Fig. 4.6. Annual relative difference of precipitation
[ALADIN-CLIMATE – HUGRID]/HUGRID [%]

4.3.4. Seasonal precipitation

Analyzing the seasonal relative difference maps of the precipitation, large differences can be noticed between the spring and summer seasons and autumn and winter seasons. In spring and summer the simulation overestimates the precipitation by 50-100 % in the Basin, and by 150-300% at the northern and eastern edge of the domain. At the same time, opposite tendencies can be seen at the south-west part of the domain. However, the forecast underestimates the autumn precipitation over about 90% of the whole area. The errors are between 10% and 30% in the centre, on the other hand, at the south-west and the north-east part of the domain exceed the -100% and the 100-150% respectively. In winter the picture is diverse and 'spotty', except for the inner Basin, where the prediction is almost perfect.

Fig. 4.7. Seasonal relative difference of precipitation
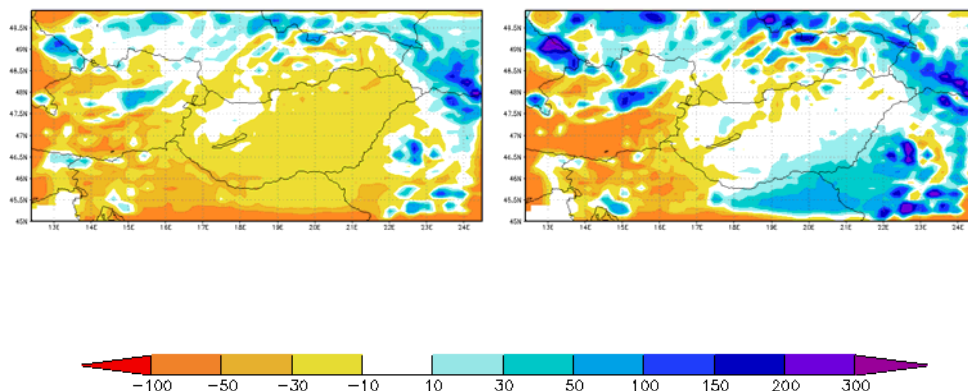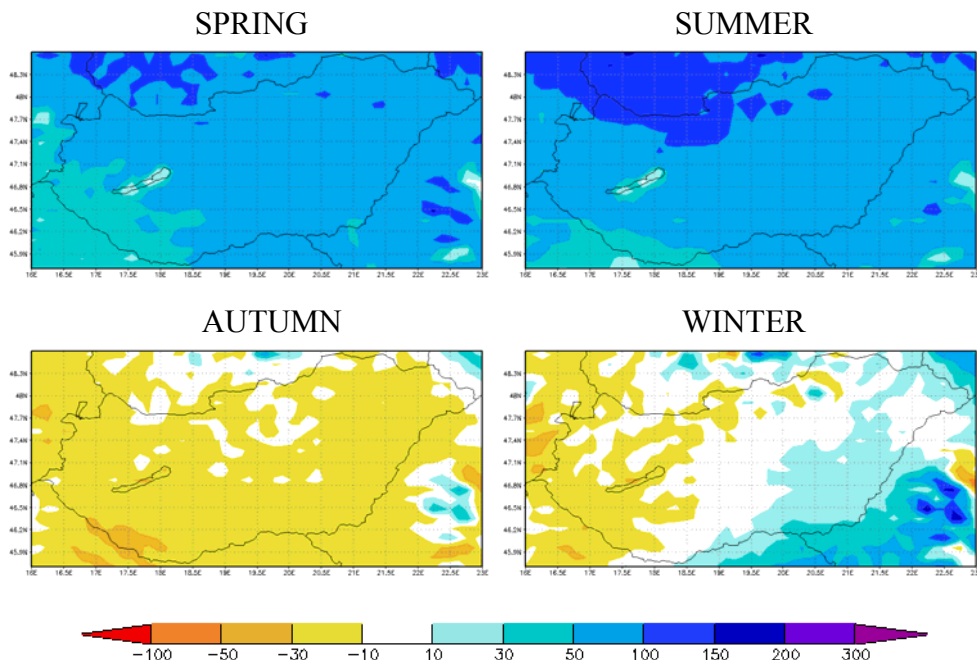*[ALADIN-CLIMATE – CRU(10')]/CRU(10') [%]*

SPRING   SUMMER

AUTUMN   WINTER

Fig. 4.8. Seasonal relative difference of precipitation
[ALADIN-CLIMATE – HUGRID]/HUGRID [%]

SPRING   SUMMER

AUTUMN   WINTER

4.3.5. BIAS and RMSE of the annual and seasonal temperature and precipitation simulations in the area of Hungary

Quantifying the results above, four tables are shown with the temperature bias (1), precipitation bias (2), temperature rmse (3) and the precipitation rmse (4) for the annual and seasonal means of the 1961-1990 period, and only for Hungary.

Certainly the numerical results confirm the general behaviour of the model as depicted from the subjective evaluation of the maps. First of all, there is no significant difference between the comparison against the CRU10' and the HUGRID datasets over Hungary. The summer season is special for temperatures (the best season) and at the precipitation (the worst season) as well. On the other hand, in winter the simulation is rather perfect in temperature and precipitation fields as well.

TEMPERATURE BIAS [C]	YEAR	SPRING	SUMMER	AUTUMN	WINTER
ALADIN-CLIMATE – CRU10'	-1.50	-2.12	-0.60	-2.66	-0.88
ALADIN-CLIMATE - HUGRID	-1.41	-2.05	-0.56	-2.28	-0.72

PRECIPITATION BIAS [mm/month]	YEAR	SPRING	SUMMER	AUTUMN	WINTER
ALADIN-CLIMATE – CRU10'	18.75	33.42	49.96	-8.52	0.17
ALADIN-CLIMATE - HUGRID	18.65	32.09	50.91	-7.45	-0.31

TEMPERATURE RMSE [C]	YEAR	SPRING	SUMMER	AUTUMN	WINTER
ALADIN-CLIMATE – CRU10'	1.55	2.17	0.89	2.71	1.26
ALADIN-CLIMATE - HUGRID	1.46	2.09	0.83	2.33	1.17

| PRECIPITATION RMSE [mm/month]	YEAR	SPRING	SUMMER	AUTUMN	WINTER
ALADIN-CLIMATE – CRU10'	20.96	35.68	54.17	14.75	11.26
ALADIN-CLIMATE - HUGRID	21.17	34.64	55.55	14.83	12.82

5. Contribution by NIMH

5. Contribution by NIMH: Localization and downscaling methods

Statistical method is an alternative for downscaling. Some sophisticated interpolation methods like procedure 927 in ALADIN have ability to give more detailed structure of some fields like temperature and sea level pressure. The RCMs could be more effective when the space resolution is reduced substantially (downscaling). In this case we may expect some improvements due to:

-   more realistic impact of land surface fields and topography,
-   reduced approximation error and improved dynamics.

That is proved by the numerical models for weather forecast and RCMs are expected to follow this practice but only if the resolution is high enough. Resolution of 50, 25 and even 15 km is not sufficient in a complex area like the domain used by NIMH. This was observed in some tests before starting operative numerical weather forecast in NIMH.

The next figure illustrates that with 50 km resolution there is no Balkan Mountains at the Balkans (isolines are in decimeters).
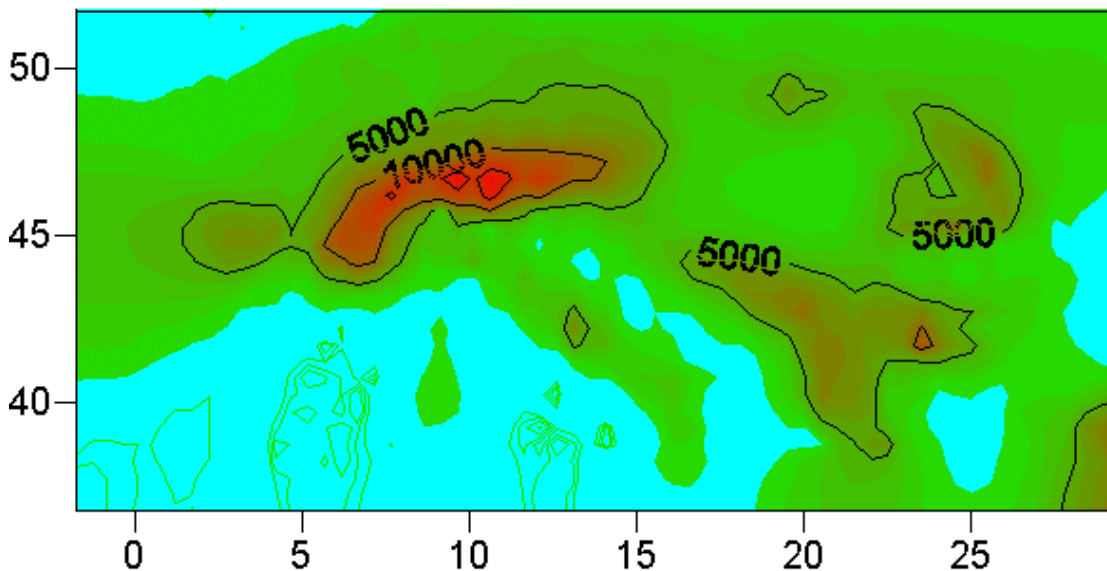
With a resolution of about 100 km of ERA40 there are no mountains, but the possibilities of a 'jump' to 10 km and reasonable response from this more detail topography was mentioned in "High resolution climate adaptation of ERA40 data over the Bulgarian domain" *Spiridonov,V., Al. Braun, M. Deque, S. Somot, Prague 2004* and "Climate version of the LAM ALADIN", *Somot S., Spiridonov V., P. Marquet., M. Deque, Prague 200)*. On the next figure we could see how resolution of 10 km for the NIMH integration domain gives crucial details:
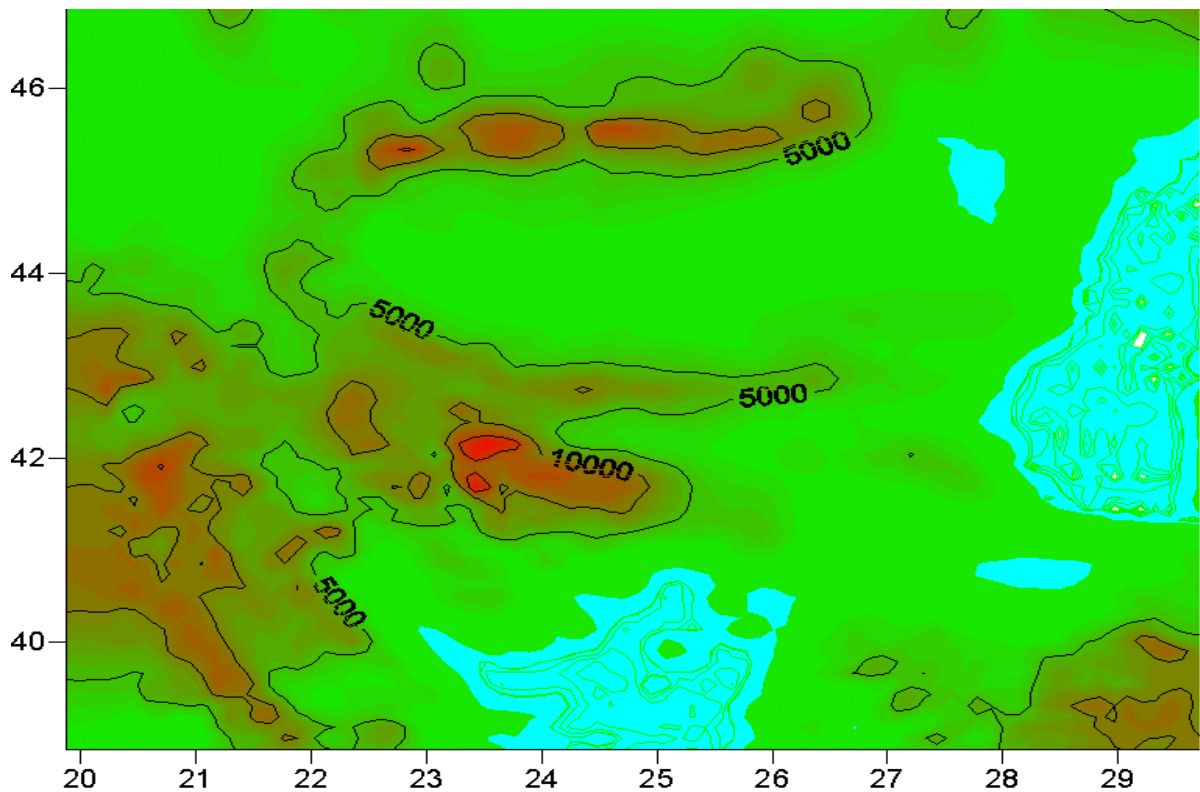
We may expect meaningful results of RCMs if the resolution respects regional features which are supposed to be important factors. We believe that 10 km resolution eventually is enough to identify the Balkan Mountains as a 'circulation barrier'. Obviously 10 km resolution is not enough to describe breeze mechanism and its onshore influence.

Verification

The problem is that we have not observation network of 10 km. The CRU data are on 50 km (even CRU 10 km is based on the same dataset) and we should downscale them or upscale results. We decided to use observations from stations situated in places affected by the land and topography characteristics and proportionally distributed. An important criterion is the quality and the period without breaks. We selected 56 stations shown in D3.2. The verification of the model ALADIN with ERA40 couplings is based on the mean values of these stations. The integration period is 1961-1990.

For such kind of verification we need localization of fields (temperature and precipitation in this case). The method was described in D3.2. The idea is to minimize the interpolation

error. Let the interpolation operator is **A**. The problem is to find a transformation **B** of the field **F** (temperature, precipitation), so that:

$$\textbf{B F - A}^{\textbf{-}}\ (\textbf{A}^{\textbf{+}}\ \textbf{B F}) = \textbf{min}$$

In this experiment as an interpolation operator **A** we used bilinear interpolation and below we present results both with linear (mentioned by **L**) localization and described method with preliminary transformation (marked by **P**).

SEASONAL MEAN TEMPERATURE C°
## (1961-1990)

TEMPERATURE
DJF
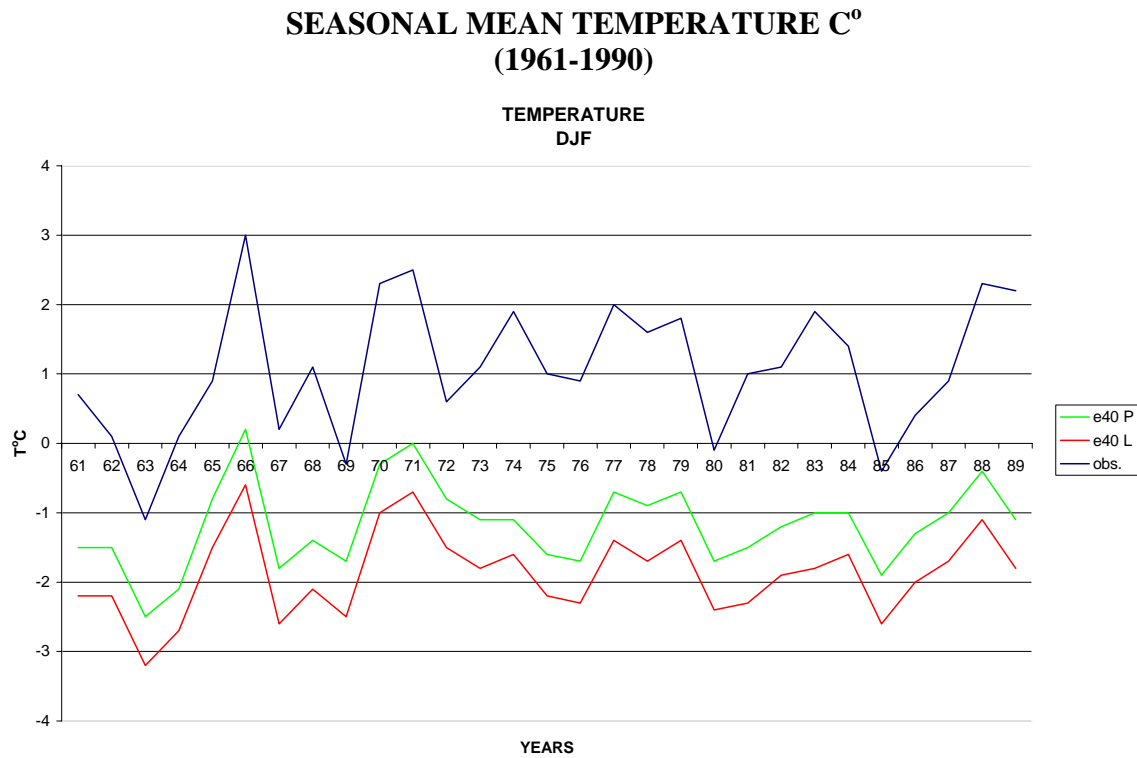
The localization using described preliminary transformation (red) leads to a less bias comparing to the direct interpolation but the simulations show cold bias for both type of interpolations. In spring (the figure below) the pattern is similar to the winter period.

TEMPERATURE
MAM
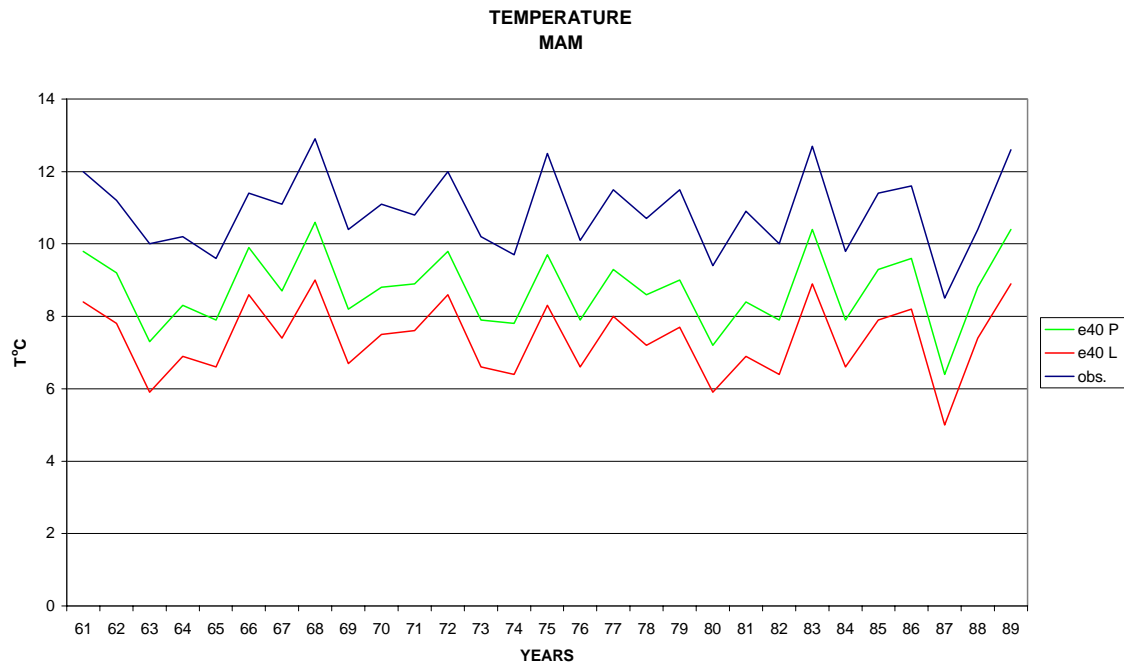
This behavior is similar in summer and autumn (next two figures).

TEMPERATURE
JJA

**TEMPERATURE
SON**
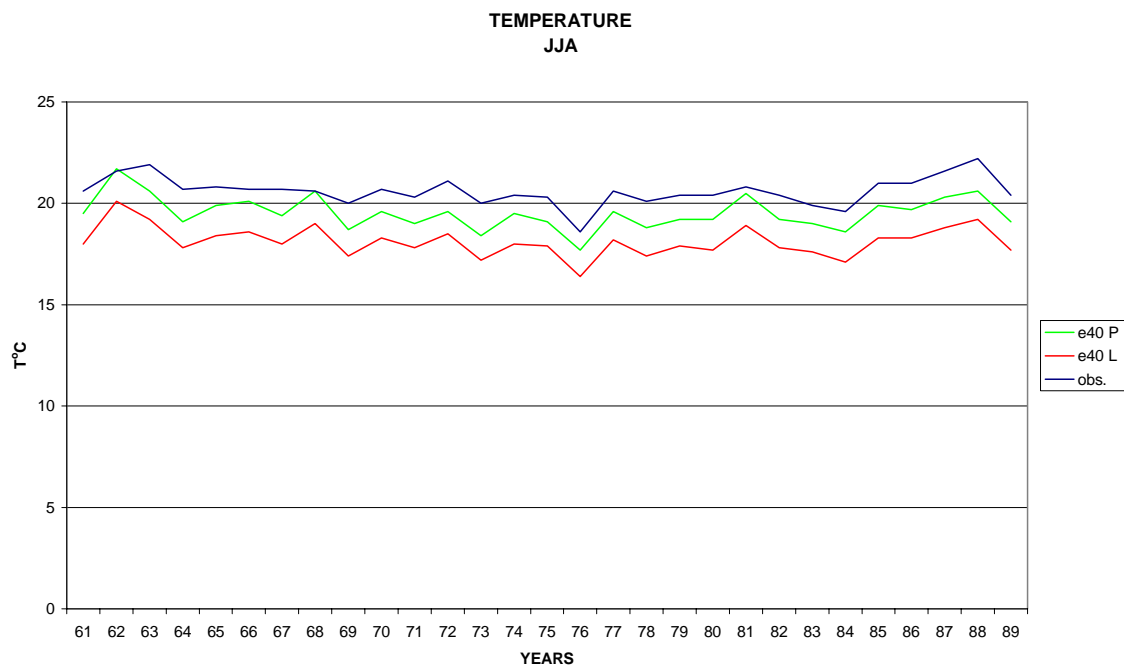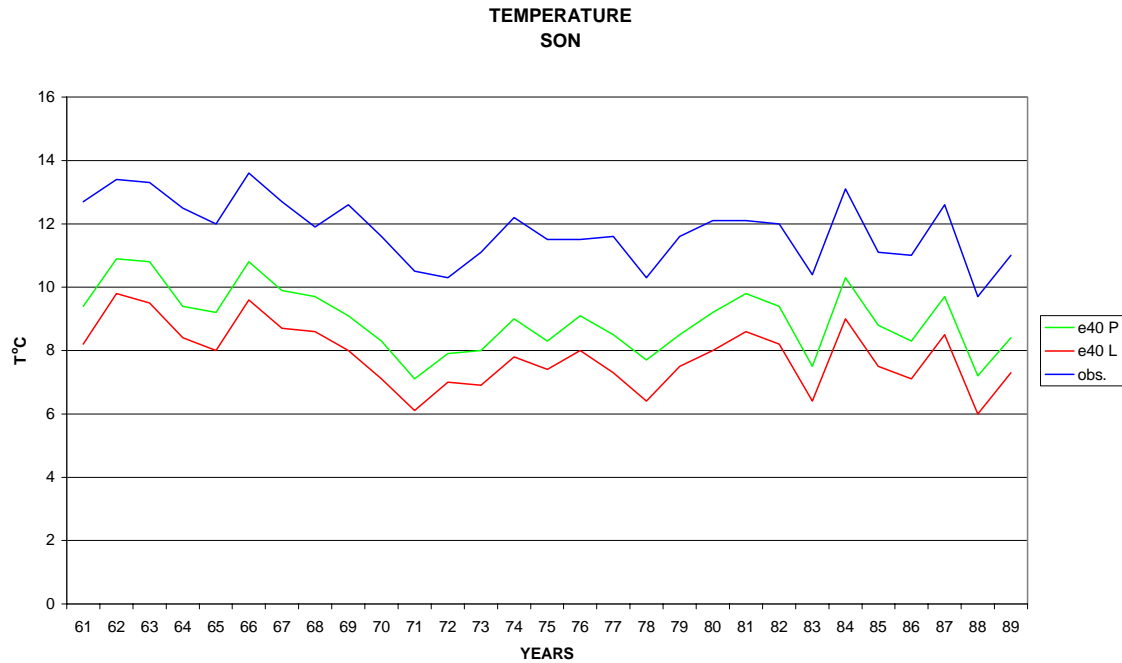
On the next tables bias and RMS are summarized for the whole period:

BIAS

	DJF	MAM	JJA	SON
E4O L	-2.950021	-3.556981	-2.547015	-3.997964
E40 P	-2.105116	-2.184690	-1.163844	-2. 848402

RMS

	DJF	MAM	JJA	SON
E4O L	2.993014	3.630809	2.713115	4.061964
E40 P	2.549860	2.223326	1.197082	2.984402

SEASONAL ACCOMOLATED PRECIPITATION (mm/m^2) (1961-1990)

The simulations for the precipitation with ERA40 are good for the winter period (the figure below)

PRECIPITATION
DJF
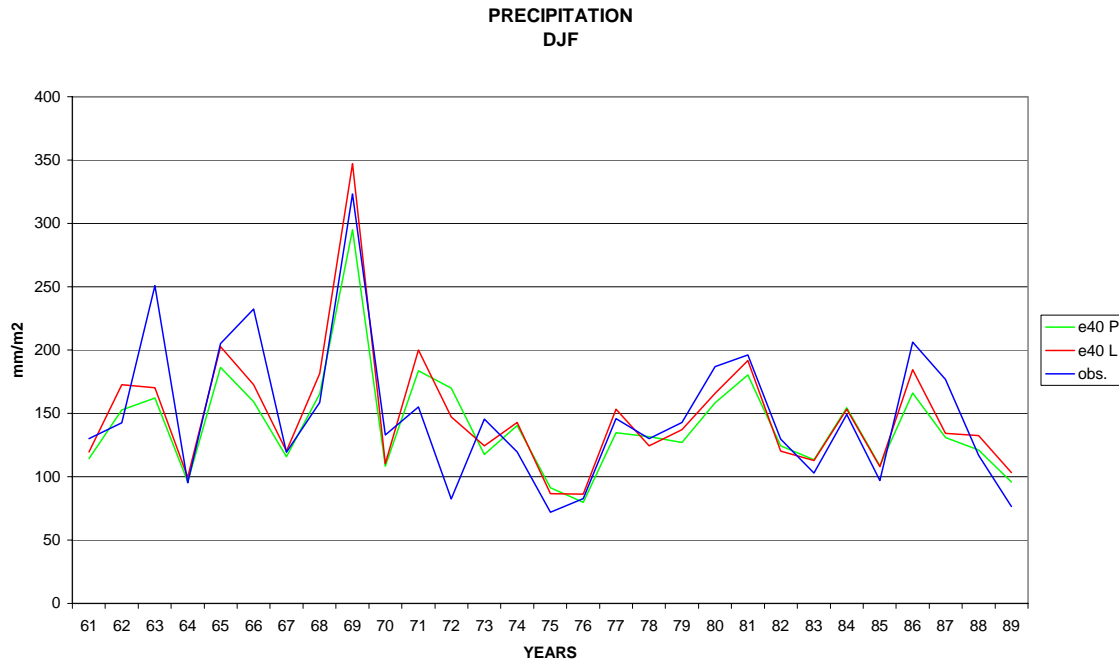
The importance of the localization method is more prominent in spring, but the simulations show wet bias.

PRECIPITATION
MAM
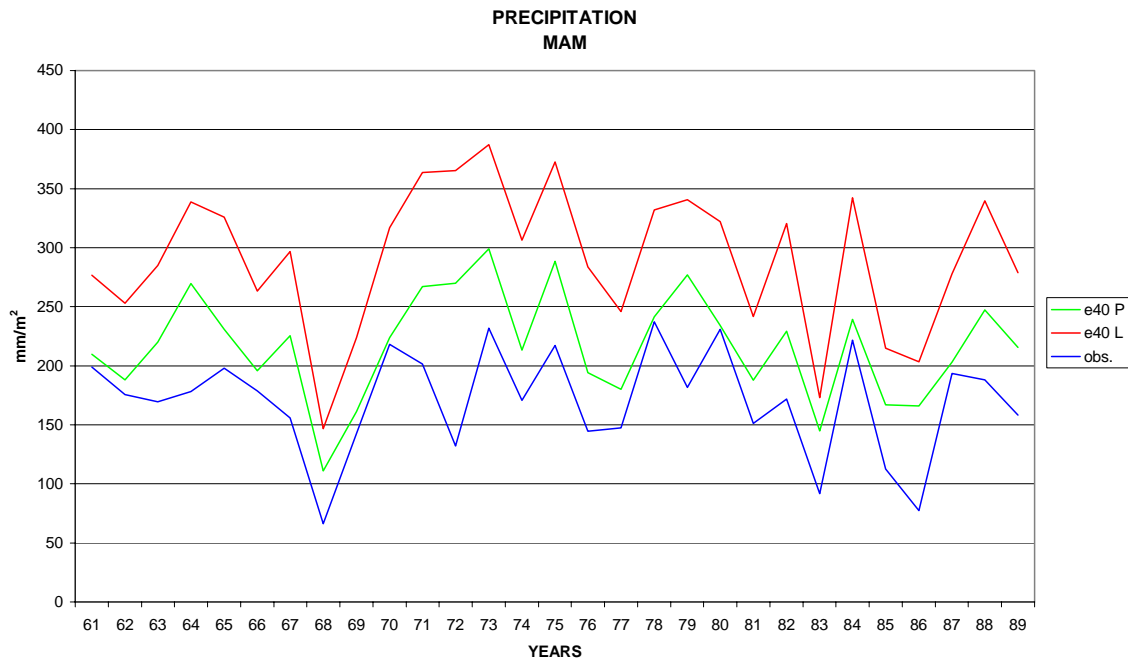
In summer the correlation with the observations is good but the bias is positive again in all stations. The localization with the preliminary transformation gains advantage over the simple interpolation method.

PRECIPITATION
JJA
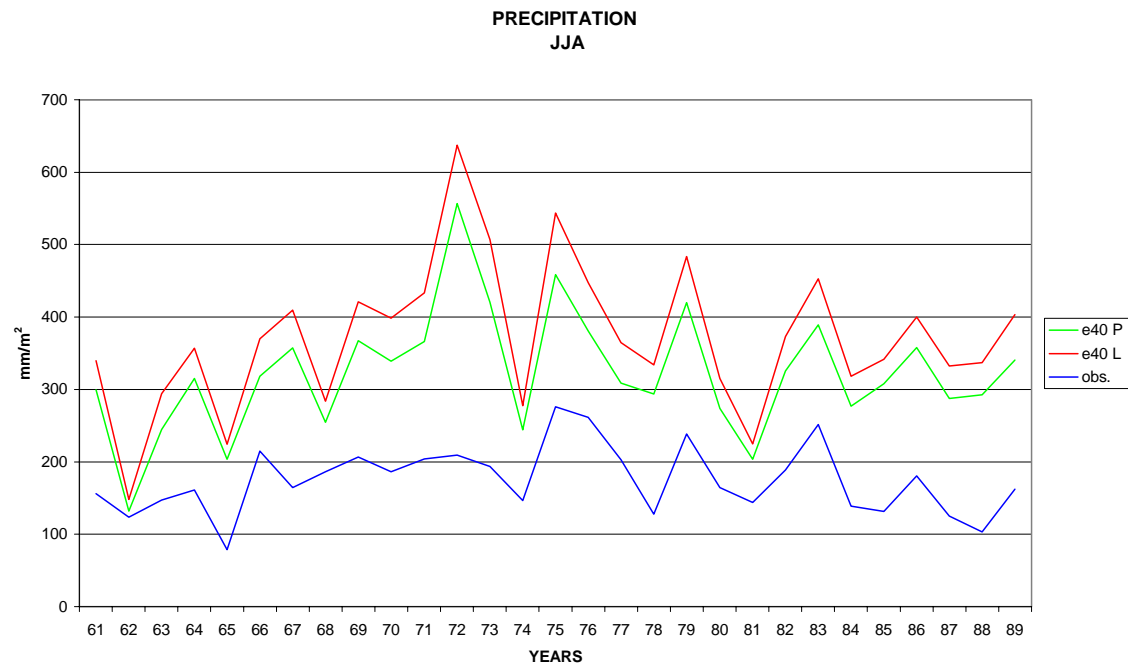
In autumn the correlation for the both localization methods is good. The bias is small and positive for the simple interpolation method and negative for the interpolation with preliminary transformation.
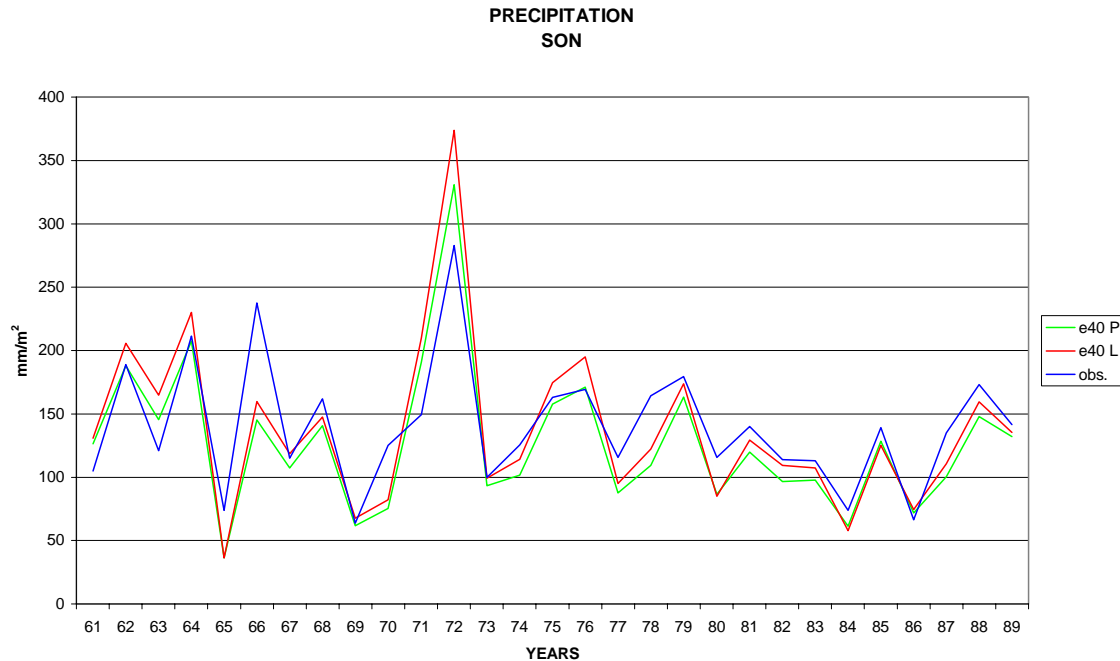
Summarizing for the simulation period:

BIAS

	DJF	MAM	JJA	SON
E4O L	-0.1409925	120.5004	200.6333	4.506385
E40 P	-7.695821	46.53494	148.4569	-8.089603

RMS

	DJF	MAM	JJA	SON
E4O L	28.97110	125.7602	209.3182	32.42067
E40 P	32.86720	56.50699	158.3000	30.42797

Conclusions

With a given RCM we have two types of downscaling - in adaptation or in climate mode respectively. In adaptation mode we use initial condition for every day (even for 6 hours) from the GCM and 'adapt' for the next 6, 12 or 24 hours. In climatic mode the initial

conditions are set only once in the beginning of the simulation. Usually the model 'settles' after one year integration. Actually the initial data are not important and this kind of simulation is called 'climate mode'.

1. ALADIN-CLIMATE model shows good correlation (seasonally year by year) with the observations in climate mode.

2. The verification of the ALADIN-CLIMATE model using the ERA40 as lateral boundary conditions shows generally cold bias for the temperature and considerably big overestimation of precipitation during spring and summer.

3. The importance of the localization method when verifying with real observation from a set of stations is illustrated in both cases, for temperature and precipitation respectively.